Naval Research Laboratory
Washington, DC 20375-5320

U.S. NAVAL RESEARCH LABORATORY

NRL/6120/MR—2023/5

Electrospun Multifunctional Composite Fibers for Improved Warfighter Insect Protection: Fiber Engineering & Bioassay Development

JEFFREY G. LUNDIN

MATTHEW D. THUM

RICCARDO CASALINI

Materials Chemistry Branch
Chemistry Division

JAVIER JIMENEZ

ASHLEY FULTON

MEGHANNE TIGHE

ASEE Postdoctoral Fellow
Washington, DC

JAMES CILEK

Navy Entomology Center of Excellence
Naval Air Station
Jacksonville, FL

JOSHUA A. ORLICKI

Polymers Branch
DEVCOM Army Research Laboratory
Aberdeen Proving Ground, MD

JUSTIN MURPHY

NICOLE HOFFMAN

High Performance Fabric Textile Facility
DEVCOM Soldier Center
Natick, MA

MELYNDA PERRY

Textile Materials Evaluation Team
DEVCOM Soldier Center
Natick, MA

August 17, 2023

REPORT DOCUMENTATION PAGE

Form Approved
OMB No. 0704-0188

1. REPORT DATE *(DD-MM-YYYY)*	**2. REPORT TYPE**	**3. DATES COVERED** *(From - To)*
17-08-2023	NRL Memorandum Report	Apr 2022 – Apr 2023

4. TITLE AND SUBTITLE

Electrospun Multifunctional Composite Fibers for Improved Warfighter Insect Protection: Fiber Engineering & Bioassay Development

5a. CONTRACT NUMBER
W74RDV22374603

5b. GRANT NUMBER

5c. PROGRAM ELEMENT NUMBER

6. AUTHOR(S)

Jeffrey G. Lundin, Matthew D. Thum, Javier Jimenez+, Ashley Fulton+, James Cilek*, Joshua Orlicki**, Justin Murphy***, Nicole Hoffman****, Melynda Perry****, Meghanne Tighe+, and Riccardo Casalini

5d. PROJECT NUMBER

5e. TASK NUMBER

5f. WORK UNIT NUMBER
9512

7. PERFORMING ORGANIZATION NAME(S) AND ADDRESS(ES)

US Naval Research Laboratory, 4555 Overlook Ave SW, Washington, DC 20375
Navy Entomology Center Excellence, Naval Air Station, Jacksonville, FL 32212
DEVCOM Army Research Laboratory, Aberdeen Proving Ground, MD 21005
DEVCOM Soldier Center, Natick, MA 01760

8. PERFORMING ORGANIZATION REPORT NUMBER

NRL/6120/MR--2023/5

9. SPONSORING / MONITORING AGENCY NAME(S) AND ADDRESS(ES)

Strategic Environmental Research and Development Program
4800 Mark Center Dr.
Alexandria, VA 22350

10. SPONSOR / MONITOR'S ACRONYM(S)
SERDP

11. SPONSOR / MONITOR'S REPORT NUMBER(S)
WP21-3053

12. DISTRIBUTION / AVAILABILITY STATEMENT

DISTRIBUTION STATEMENT A: Approved for public release; distribution is unlimited.

13. SUPPLEMENTARY NOTES

*Navy Entomology Center of Excellence, Naval Air Station, Jacksonville, FL 32212, **Polymers Branch, DEVCOM Army Research Laboratory, Aberdeen Proving Ground, MD 21005, ***High Performance Fabric Textile Facility, DEVCOM Soldier Center, Natick, MA 01760, ****Textile Materials Evaluation Team, DEVCOM Soldier Center, Natick, MA 01760, +ASEE Postdoctoral Fellow at U.S. Naval Research Laboratory, 4555 Overlook Ave. SW, Washington, DC 20375-5320

14. ABSTRACT

We report on progress made in year 2 of WP21-3053 on the development of novel multifunctional fibers for the controlled delivery of environmentally friendly, low toxicity insect repellents encapsulated in the core of polymer fibers via electrospinning and dry jet wet spinning to demonstrate feasibility for transition. Individual fibers were engineered by electrospinning, as well as scalable extrusion methods, to exhibit one or more functionalities providing multiple approaches to produce yarn and/or fabric composites for environmentally sustainable multifunctional textiles.

15. SUBJECT TERMS

Electrospinning, Dry jet wet spinning, Fibers, Insect repellents, Multifunctional composites, Textiles, Nylon

16. SECURITY CLASSIFICATION OF:			**17. LIMITATION OF ABSTRACT**	**18. NUMBER OF PAGES**	**19a. NAME OF RESPONSIBLE PERSON**
a. REPORT	**b. ABSTRACT**	**c. THIS PAGE**			Jeffrey G. Lundin
U	U	U	U	72	**19b. TELEPHONE NUMBER** *(include area code)* (202) 404-2529

Standard Form 298 (Rev. 8-98)
Prescribed by ANSI Std. Z39.18

This page intentionally left blank.

Table of Contents

Table of Figures

Table of Tables

Abbreviations

ARL	Army Research Laboratory
ATR-FTIR	Attenuated Total Reflectance Fourier Transform Infrared
DCM	Dichloromethane
DEET	*N*,*N*-Diethyl-*meta*-toluamide
DSC	Differential Scanning Calorimetry
E_a	Activation Energy
EPA	Environmental Protection Agency
FA	Formic Acid
GC-MS	Gas Chromatograph / Mass Spectroscopy
h	hour
HSP	Hansen solubility parameter
IR	Infrared
kV	Kilovolt
MSM	methylsulfonylmethane
NRL─DC	Naval Research Laboratory, Washington D.C.
P(AN-VC)	poly(acrylonitrile-co-vinyl chloride)
P(AN-VC)/DEET	P(AN-VC)-DEET composites
PET	poly(ethylene terephthalate)
PLLA	poly(L-lactic acid)
pTSAm	*para*-toluenesulfonamide
RED	Relative Energy Difference
rPET	recycled PET
SC	Soldier Center
SEM	Scanning Electron Microscopy
SLN	Solid lipid nanoparticles
TA	Tannic acid
TFA	Trifluoroacetic acid
TGA	Thermogravimetric Analysis
VOCs	Volatile organic compounds
wt%	Weight Percent

Keywords

Electrospinning, dry jet wet spinning, fibers, insect repellents, multifunctional composites, textiles, nylon

Acknowledgements

In support of this joint initiative, the authors wish to thank the following parties: SERDP Program Office for financial support; the Office of Naval Research and the US Naval Research Laboratory.

This page intentionally left blank.

1. Abstract

1.1. Introduction and Objectives

We report on progress made in year 2 of WP21-3053 on the development of novel multifunctional fibers for the controlled delivery of environmentally friendly, low toxicity insect repellents encapsulated in the core of polymer fibers via electrospinning and dry jet wet spinning to demonstrate feasibility for transition. Individual fibers were engineered by electrospinning, as well as scalable extrusion methods, to exhibit one or more functionalities providing multiple approaches to produce yarn and/or fabric composites for environmentally sustainable multifunctional textiles. Our specific objectives for this reporting period were 1) evaluate the potential efficacy of dual repellent fiber designs, 2) develop and validate a bioassay for repellent-loaded fibers, and 3) identify fiber designs that are compatible with transition to scalable production methods.

1.2. Technical Approach

This program is organized into 4 tasks. First, dual insect repellents (Task 1) are incorporated into electrospun nylon fibers to evaluate potential synergistic effects uniquely enabled by the electrospinning process. Second, electrospun fibers are physically spun into threads to demonstrate direct transition capability for improved performance for multifunctional uniform applications (Task 2). Third, insect repellent composite fiber designs developed under Tasks 1 and 2 are transitioned to conventional fiber drawing techniques and efficacy (mechanical, release properties) compared to demonstrate feasibility for scale-up (Task 3). Finally, additional additives (fire retardant and antimicrobial) are separately incorporated into the most successful insect repellent designs via electrospinning to demonstrate potential for dual-functionality (Task 4).

Manuscript approved August 15, 2023.

Ultimately, this research is designed to produce several different fiber designs with well proven transition potential that could be used to design new multifunctional fabrics.

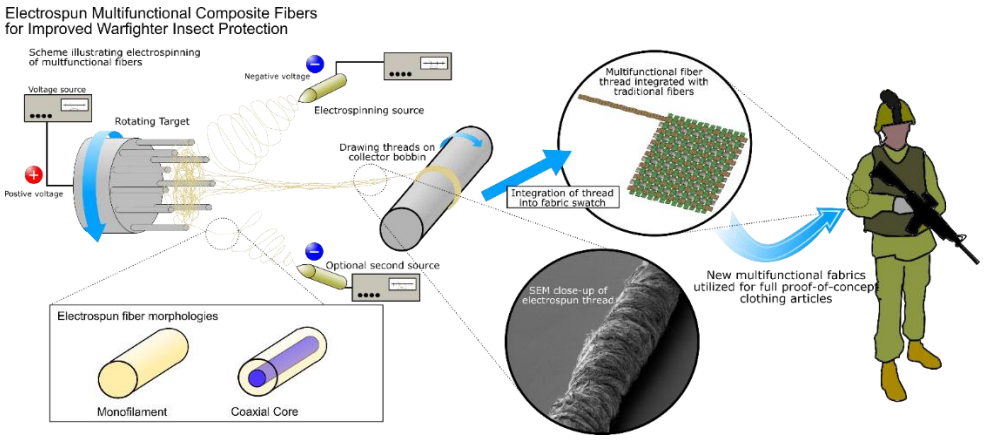

Figure 1. Conceptualization of direct development path of monofilament and coaxial electrospun fibers to functional webs, patches, and potentially textiles.

The flexibility afforded by electrospinning provides the opportunity for the generation of a library of multifunctional fibers with different additives, chemistries, and physical properties (Figure 2, left). Individual fibers may be tuned to encapsulate varying functionalities and at different concentrations or monofunctional fibers may be blended to form multifunctional fibers or yarns depending upon the use case. This approach has the potential to enable new textile manufacture methods that generate numerous multifunctional products that could impact multiple applications, including intelligently designed ‘smart’ uniforms, including garments with localized behavior (e.g., collars with high loading of insect repellent). Furthermore, electrospinning can serve as a testbed technology to allow for rapid prototype and demonstration of the coaxial designs, from which more conventional coaxial processing techniques can be easily adapted for transition to large scale production (Figure 2, right).

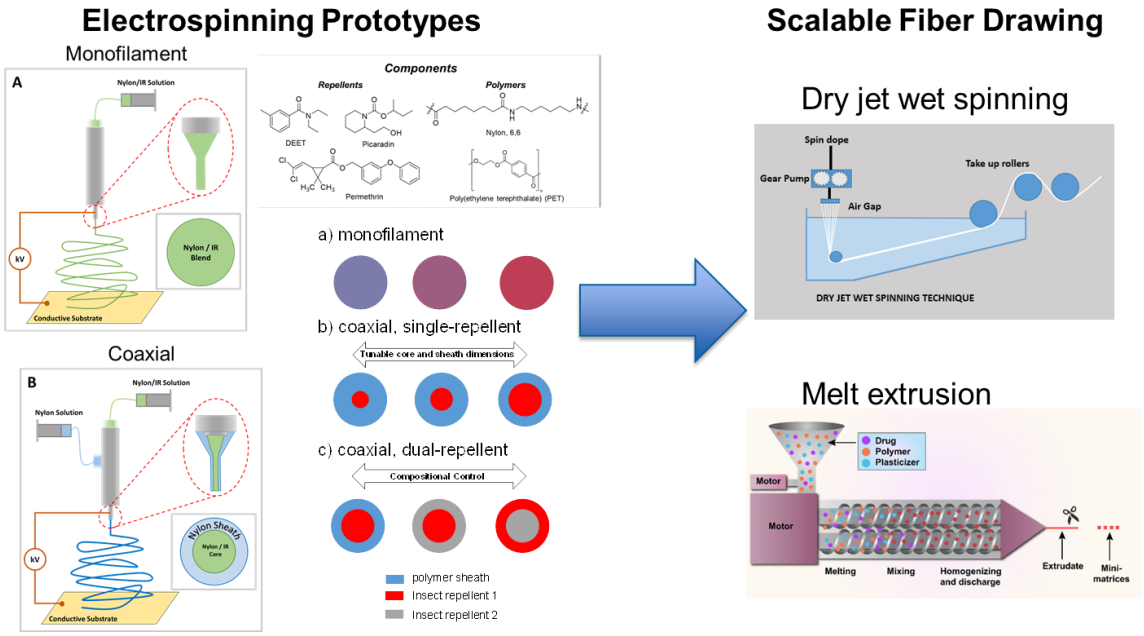

Figure 2. Transition of fiber designs enabled by electrospinning (left) to more scalable fiber production methods, dry jet wet spinning and melt extrusion (right).

1.3. Results

In year 2, we have made substantial progress in Tasks 1, 3, and 4, which correspond to electrospun prototyping, scalable extrusion, and multifunctional fibers, respectively. In Task 1, we developed mixed insect repellent-doped recycled polyethylene terephthalate (PET) electrospun microfibers and demonstrated their efficacy using a novel live insect bioassay specifically designed for insect repellent loaded textiles. In task 3, we made progress in two parallel scalable fiber fabrication pathways, dry jet wet spinning and melt extrusion. We identified and employed the benefits of dry jet wet spinning, which extrudes polymer gels at relatively low temperatures that enables the incorporation of volatile repellents, to a novel polymer-DEET gel formulation that has significant promise to serve as a fiber core, as well as standalone repellent material. For melt extrusion, we identified a promising melt depressant that effectively lowers the processing temperature of nylon to enable compatibility with insect repellents. Towards Task 4, we designed,

formulated, and tested flame retardant tannic acid-nylon fibers that showed natural product tannic acid was effective as a fire-retardant additive for nylon. We will build upon these findings in year 3 to incorporate insect repellency for a multifunctional fiber proof of concept.

1.4. Benefits

The encapsulation of insect repellent (i.e., picaridin, DEET) into textile fibers via a bottom-up approach affords the potential to create fabrics and garments that offer long-term protection to the warfighter from insect-borne diseases. Incorporation of the active materials into the core of the fibers will greatly enhance the durability of these functionalities to laundering, especially when compared with surface treatments, strongly reducing the current health hazards present for surface treated fibers and increasing their environmental sustainability. The insect repellent fibers that will result from this proposal have the potential to greatly reduce environmental and health risks during their lifecycle by 1) increasing the longevity of functionalities after laundering, 2) reducing direct skin contact of active additives by encapsulation within the core of a benign material, and 3) generating novel fibers from which textiles and garments could be intelligently designed with functionalities localized and limited only to the areas in which they are needed.

In this reporting period, we present several advancements in the program that have potential to serve as standalone insect repellent materials, will enable future development insect repellent loaded fibers and textiles, and provide significant contribution to the field. The nonwoven fibrous mats sourced from recycled PET consumer goods have the capability to function as patches for long-term repellent release to repel biting arthropods from exposed skin. Furthermore, the high affinity between DEET and PET we identified will be leveraged in the design of future filaments. Our development and demonstration of a novel bioassay specifically

designed to evaluate the repellency of insect repellent loaded fibers and textiles will have significant implications for providing live insect performance on materials developed in Y3 of this program, as well as provide new and useful methods to others in the field. Our design and formulation of insect repellent loaded-polymer gels has potential for significant impact as standalone insect repellent materials (passive-release or thermally induced repellent beads, strings, gels), as well as to serve as a highly loaded core in bicomponent fiber designs. Importantly, the gel designs are compatible with dry jet wet spinning, which is a scalable, manufacturing compatible extrusion method. We also identified a promising melt depressant to lower the processing temperatures of nylon to enable volatile repellent incorporation to improve the compatibility of insect repellents with conventional melt extrusion manufacturing, which represents a promising transition pathway for textile applications.

2. Background

2.1. Mosquito-borne disease

Mosquitos are considered one of the world's deadliest creatures causing over 700,000 deaths per year as vectors for which deadly diseases such as Zika, malaria, and West Nile can spread[1-3]. Over a billion animals and humans are infected yearly, with malaria as the most common mosquito-borne disease. In 2021, approximately 247 million people were infected with malaria, which caused 619,000 deaths[4]. Elimination of malaria and other mosquito-borne diseases requires preventative measures to stop transmission. The World Health Organization provides insecticides-treated mosquito nets and indoor insecticide spraying for the homes of people countries heavily impacted by malaria[4]. Preventative strategies for indoor protection such as long-lasting insecticidal bed nets and indoor residual spraying have been effective in reducing *Plasmodium falciparum* infection in endemic Africa by half and the incident of clinical disease by 40 % between 2000 and 2015.[5] However, outdoor environmental protection is regulated to topical treatment directly to the skin, such as insect repellent aerosol-type sprays and creams[6]. These measures are effective, but concerns of skin permeation[7], water pollution[8], and short efficacy time due to evaporation[9] brings about a need for an indirect way of protection. As a result, efforts to increase insect repellent/insecticide efficacy times have included physically entrapping the substrate into a polymeric material for outdoor protection.[10]

2.2. Current Approaches to Extended Insect Repellent Release

Common commercially available synthetic based insect repellents contain *N*,*N*-diethyl-meta-toluamide (DEET) or 1-(1-Methylpropoxycarbonyl)-2-(2-hydroxyethyl)piperidine (picaridin)[11]. The EPA also recognizes IR3535 and oil of lemon eucalyptus as biopesticides used

as natural-based repellents[12]. Topical repellents allow for mobile protection, but require reapplication for extended protection. For example, picaridin is a volatile compound with an estimated half-life of 5 hours at a concentration of 25%[13]. Repellent sprays generally work in the vapor and liquid phases, and their efficacy lifetime is limited by evaporation and absorption. DEET is a multi-modal repellent, repelling through olfactory avoidance, contact, and ingestion[14]. The vapor barrier of picaridin disrupts the insect's olfactory sense and taste preventing contact[15]. Encapsulation of repellents have shown to enable the extended release of repellents[16-17]. For example, solid lipid nanoparticles (SLN) have a high capacity of repellent loading but requires direct contact with the skin[18]. Polymer-based encapsulations have proven most effective while limiting contact with the skin. The release rate of these systems depend on diffusion from the polymer matrix. Polymeric microcapsules consist of insect repellent encased in a spherical polymer sheath. Kadam and coworkers synthesized polyurethane microcapsules with DEET that had a significant reduction in the release rate of DEET[19]. Synthesis of polymeric fibers containing insect repellent have been accomplished through extrusion[20] and melt spinning[21]. However, electrospinning provides a facile and quick method to identify fiber formulations for extended repellent release.

Electrospinning polymer materials have been effective employed in drug delivery[22] and to extend the release of insect repellents[23-24]. The synthesized fibers can quickly be tested for the composition as well as release of repellents. Monofilament nylon nanofibers was shown to have extended release of DEET with calculated half-life as high as 70 h[23]. Picaridin has also been utilized in the synthesis of fibers and was observed to have extended release of the repellent[24]. There is a wide range of materials used in electrospinning. Munoz and coworkers synthesized cellulose–based nanofibrous mats for insect repellent activity[25] using the biorepellent citriodiol.

Biodegradable electrospun nanofibers have also been fabricated from poly(L-lactic acid) (PLLA) with incorporation of DEET[26]. Reuse of a material has promise in the study of insect repellent-doped fibers.

Polyethylene terephthalate (PET) is a class of polyesters widely used in the food and beverage industry[27]. The polymer material provides transparent, rigid packaging that can be produced at a low cost. As a result, the food and beverage industry use PET to package many single-use products. Unfortunately, the increased use of PET has become an escalating environmental problem[28]. The United States generates the largest amount of plastic waste in the world at 44 metric ton produced in 2019[29]. Recycling PET bottles provides a solution to an environmental problem while also being cost effective[30].

2.3. Polymer Gels

Passively-controlled substrate release has most commonly been investigated for in vivo drug delivery systems through gelled polymer morphologies.[31-32] The high degree of free space in gelled microstructures compared to paracrystalline materials allows for efficient substrate loading, thus making gels the preferred loading vessel for in vivo drug delivery systems.[33] Physical gels give the added benefit of thermo-reversal properties through the formation and deformation of microcrystals at polymer chain entanglement junctions. At temperatures above this gel point, processes such as injection molding or fiber spinning can form consumer products such as bracelets or textiles without requiring a crosslinking/curing stage. Moreover, once depleted of their substrate the residual polymer can then be recycled due to maintaining a linear structure thus forming a circular economy.

Physical gels are a miscible polymer and solvent system that exhibit a storage modulus

greater than the loss modulus (G”/G’ = tan(δ) ≤ 1) at 1 Hz.[34] The gel point where tan(δ) = 1 is dependent on variables such as polymer concentration, polymer molecular weight, polymer/solvent types, and temperature. The insect repellent loading in a physical gel is maximized if the repellent acts as the gelling solvent. Therefore, the polymer and insect repellent must be miscible with one another. Hansen Solubility Parameters (HSPs) quantify chemical affinities through a tri-coordinate characterization that has been proven to determine polymer/solvent miscibility.[35]

2.4. Flame Retardant Polymer Fibers

Oftentimes, polymer morphology informs application. The development of high-performance polymer fibers has been a driver of applications including textiles and biomedicine, but there are many applications, including textiles, and air filtration, that require flame retardancy. As a processing technique, electrospinning is a facile and versatile method of preparing nanofibrous materials from a library of different polymer scaffolds and additives ranging in scale from nm to microns[36]. Fibers can be prepared with varying morphologies, including core-sheath, multi-core sheath, beaded, hollow, porous, webbed, and more[37-42]. The most common electrospinning process uses high voltage applied to the end of a needle tip, through which a polymer solution is passed using a syringe pump, to accelerate the newly formed polymer jet towards a grounded collector plate. During this process, rapid solvent evaporation results in the formation of polymeric fibers which are then collected on the grounded plate. The application of electrospinning to flame-retardant polymeric materials has been used for textiles, coatings, and, of significant recent interest, membrane separators for lithium-ion batteries[43-47]. A major drawback of many flame-retardant materials is environmental and exposure concerns, especially when

dealing with textiles. Polyphenols have shown significant promise as a family of non-toxic biomolecules used as naturally occurring flame retardant materials[43, 48-49]. Polyphenols are excellent char-formers, good radical scavengers making them ideal flame-retardant materials, however, they rapidly degrade under high temperature making it difficult to fabricate polymer composites using traditional melt-extrusion and melt-forming methods[48]. Of the polyphenols currently studied, tannic acid (TA), a naturally occurring polyphenol, has high char-forming tendency due to its network of aromatic rings and is an exceptional radical-scavenger[50]. Upon heating to the point of thermal decomposition (ca. 200-230 °C), tannic acid acts as an intumescent material. Decomposition of the ester linkages results in the release of CO_2 and the pyrolysis of the aromatic rings leads to the formation of a char layer thus insulating and underlying areas.

3. Materials & Methods

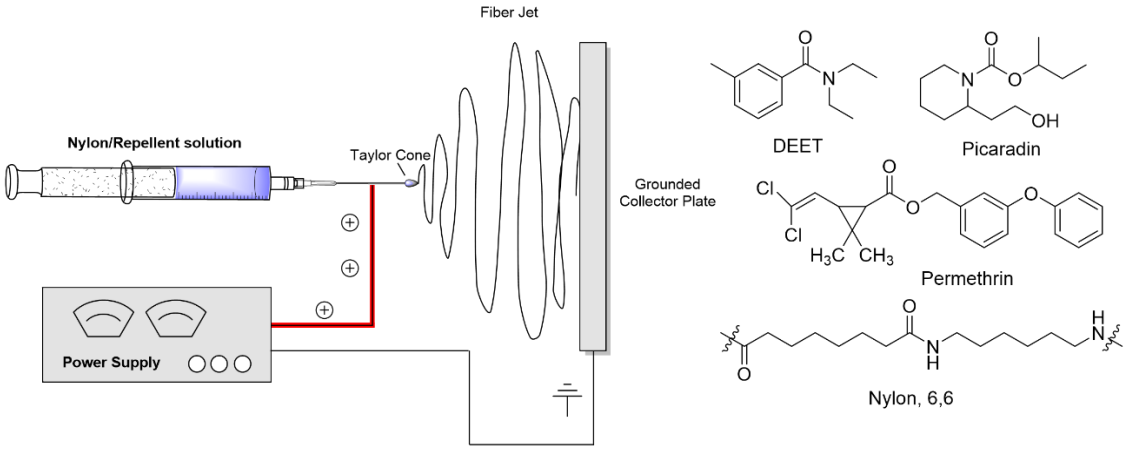

Figure 3. (Left) A general depiction of an electrospinning setup. High voltage is applied to a needle tip through which a nylon/repellent solution is pumped. At the Taylor cone formed at the needle tip, the solvent evaporates as the polymer jet accelerates towards the collector plate. The result is a non-woven mat of polymeric nanofibers. (Right) The chemical structures of common insect repellents and representative textile polymer, nylon 6,6.

Materials. Polyethylene terephthalate (PET) was recycled from consumer soft drink bottles obtained from the Coca Cola and Pepsi Company. The bottles were rinsed thoroughly first with distilled water, then methanol (Sigma-Aldrich, 99% purity), and allowed to dry. Trifluoroacetic acid (TFA) and dichloromethane (DCM, HPLC grade) were purchased from Fischer Scientific and used as received. *N*,*N*,-diethyl-meta-toluamide (DEET) was provided by TCI America, and 1-(1-methylpropoxycarbonyl)-2-(2-hydroxyethyl)piperidine (picaridin) was purchased from MedChemExpress (Monmouth Junction, NJ). Nylon 6/6 (nylon) was obtained from Aldrich (429171-1KG), tannic acid (TA) was provided from Fisher Scientific, and Formic acid (88%) was provided by Fisher Scientific. All materials were used as received without further purification.

Electrospinning monofilament PET fibers. Solutions of recycled PET (rPET) were prepared by cutting the drinking bottles into 1 x 1 cm pieces. A mixture of 30% TFA and 70%

DCM by weight was made. The rPET pieces were added to the solution at 10 rel. wt% concentration. DEET, Picaridin or a mixture of 1 to 1 DEET/Picaridin was added to the rPET solution to achieve the desired concentration with respect to rPET (0, 10, 15, 30, 40, 50, 54, 60, 70 wt%), Table 1. Solutions were sealed and mixed for 24 h at 20 °C to obtain complete homogenous mixtures. For mixtures containing 60 and 70 wt% DEET, heating at 60 °C overnight (18 h) was required. After dissolution, solutions were stored at 2 – 4 °C and warmed to room temperature before use.

Monofilament fibers were fabricated through electrospinning on a custom-built system. The polymer solutions were loaded into a 10 mL syringe equipped with a 22 gauge needle. A New Era Pump Systems syringe pump (NE-300) was used to dispense the solution horizontally toward a grounded collector. The needle was set at a distance of 12 cm from grounded collector. Accelerating voltage was set to 12 kV by a Bertan Series 205B high voltage power supply. Fibers were collected onto aluminum foil as nonwoven mats. For live insect testing, fibers were collected for 45 min. onto a 10 x 10 in. metal wire screen. All nonwoven mats were evaluated following 24 h residence at room temperature (18 °C) to afford solvent removal.

FR Nylon Solution Preparation. Nylon solutions were prepared by dissolving 1.25 g nylon in formic acid up to a total mass of 10 g. To this, TA was added to achieve the appropriate concentration with respect to nylon (0, 10, 30, 50, 75, 100 rel. wt%). All repellent concentrations are reported as a relative wt% (rel. wt%) with respect to nylon. The theoretical concentration of TA in the electrospun fibers is given in Table 1. After the polymer and repellent were thoroughly mixed, the solution was sealed and heated to 50 °C overnight in a block heater to completely dissolve the contents. Sealed solutions were kept for no more than a week at 2 – 4 °C and allowed to warm to room temperature before electrospinning.

Electrospinning FR Nylon Fibers. Monofilament electrospinning was performed on a custom-built system using a New Era Pump Systems syringe pump (NE-300) oriented horizontally towards a grounded collector. The electrospinning solution was loaded into a 5 mL syringe with a 22-gauge needle. Fibers were electrospun at 0.9 $mL \bullet hr^{-1}$, 20 – 22 °C, and a relative humidity of <35 %. The needle was set at distance of 15 cm away from the collector horizontally and the voltage between the needle and collector was set to 15 kV for samples containing 0 – 50 rel. wt% TA and 19 – 20 kV for samples with >50 rel. wt% TA. Voltage was supplied by a Bertan Series 205B high voltage power supply. Fibers were collected on aluminum foil for 2 – 6 hours.

Scanning Electron Microscopy. The morphology of electrospun monofilament fibers was characterized by field emission scanning electron microscope (SEM) on a JEOL JSM-7600F (Peabody, MA). Operating voltage was set to 5 kV. Samples were sputter coated with at least 3 nm of gold prior to SEM analysis using a Cressington 108 auto sputter coater equipped with a MTM20 thickness controller. Fiber thickness was determined using ImageJ software ($n \geq 100$).

Optical Microscopy. Optical microscopy was performed using a Zeiss Axio Imager 2. Images were taken using EC Epiplan-Neofluar 5−100× objectives and processed using Zen Core software (Zeiss, Oberkochen, Germany). Samples were prepared on glass slides and were analyzed in reflection or transmission mode.

Thermal Analysis. Analysis of release kinetics and fiber composition was measured by thermogravimetric analysis (TGA) on a TA Instrument Discovery TGA using platinum pans (100 μL). Thermal decomposition was evaluated by heating ramps performed at a heating rate of 10 °C/min to 600 °C. Kinetic measurements were deduced from isothermal decay curves performed in a nitrogen atmosphere at 60, 80, and 100 °C for 300 min. Isothermal curves were fit to nonlinear decay models using Origin software.

Thermal Analysis of FR Nylon Fibers. Analysis of release kinetics and fiber composition was characterized by thermogravimetric analysis (TGA) on a TA Instruments Discovery TGA using platinum pans (100 µL). Heating ramps were performed at a heating rate of 10 °C•min^{-1} to 600 °C. For analysis in air, the flow gas was switched from N_2 to air at 50 °C. The char yield was measured as the percent of residual mass remaining at 600 °C.

ATR-IR Analysis. Compositional analysis of electrospun nanofibers was evaluated using an attenuated total reflectance-Fourier transform infrared (ATR-FTIR) spectrometer from Thermo Scientific (Nicolet iS50-FTIR spectrometer) equipped with an iS50 ATR attachment and Ge crystal. Background and sample spectra consisted of 128 scans averaged together with 4 cm^{-1} resolution at a scanner velocity of 10 kHz.

Headspace analysis and method. To detect the volatile organic compounds (VOCs) in the headspace of rPET/DEET/picaridin fibers, a 7890B/5977B Agilent GC-MS coupled with the 7697A Agilent Headspace Sampler (Agilent Technologies, Santa Clara, CA) was used for analysis. The GC-MS was equipped with a 30 m x 0.25 mm i.d. x 0.25 mm, Rxi-5MS column (Restek, Bellefonte, PA). The sample subjected to headspace analysis was rPET-54-DP monofilament fibers produced via electrospinning. Approximately 2 mg of fibers were prepared, rolled into a ball, and placed into a 20 mL Agilent headspace vial equipped with a crimp cap. The fibers were allowed to sit at room temperature (22 °C ± 3°) for 2 h. Prior to headspace extraction, the vial was allowed to equilibrate at 90 °C for 25 min while shaking at 50 shakes/min in the headspace sampler, and then followed by 30 s injection to the injection loop set at 90 °C. The sample was transferred to GC-MS via transfer line set to 100 °C, the analytes flowed at a rate of 20 mL/min. The GC column oven began at 40 °C, was held for 30 s, increased to 250 °C at 40 °C/min, and finally held at 250 °C for 1 min. The mass scan range m/z 40-300 and the transfer line to the MS was 250 °C.

Hansen Solubility Parameters (HSP). Diffusion kinetics between polymer and substrate were quantifiably interpreted through Hansen Solubility Parameters (HSPs) analysis. HSPiP software obtained from Hansen-Solubility website (https://www.hansen-solubility.com/HSPiP/) was used to perform analysis.

Live Mosquito Bioassay. Three- to five-day old insecticide-susceptible female *Aedes aegypti* (ORL strain) were used in all evaluations. Laboratory bioassay methods used a modification of Jiang et al.[51] in 3.8 diameter by 30.5 cm clear glass cylinders. Treatments consisted of either 50% (AI) DEET, picaridin, or a 1:1 mixture of both impregnated in 10% PET fibers. A 4.5 cm diameter hole punch was used to remove standardized disc samples from each textile for testing. Three samples were removed from each textile mat (mats N=2). Each excised disc was then separately placed into an open ended 4.5 diameter x 1.0 cm translucent polyethylene end cap (SF-16, Caplugs, Buffalo, NY) and placed over one end of the glass cylinder. An average of about 15 non-blood fed mosquitoes were then mouth aspirated into each cylinder (Figure 4).

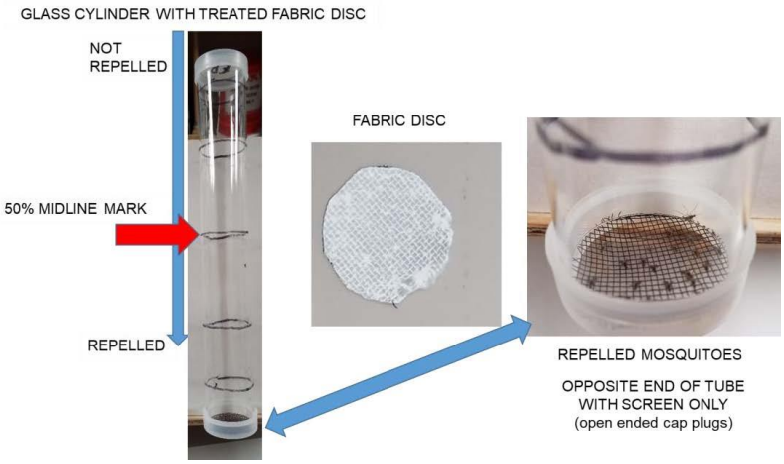

Figure 4. Diagram of bioassay using live insects.

Once mosquitoes were introduced into each tube, a similar sized metal 1 x 1.2 mm mesh window screen disc with endcap was placed on the opposite end to prevent escape of mosquitoes

and provide ventilation. Initially, all cylinders were positioned horizontally on a table until the start of testing. Once mosquitoes were transferred to all tubes, they were positioned at a 45° incline[51-52] with the textile disc at the top of the cylinder. Controls consisted of 10% PET only, as well as the metal window screen the latter used as a negative control. Testing started at approximately 0700 and data recorded at 10, 15, 30 min, then hourly through 8 h of continuous exposure in tubes. Mosquitoes located on or beyond the midline of the tube were scored as repelled based on the criteria of Jiang et al.[51] To determine residual effectiveness of treatments, testing was conducted at 0, 24 h, and weekly intervals thereafter for 4 wks. Between these time intervals all discs were stored in separate clear plastic polyethylene bags at ambient room temperature in a windowless laboratory under continuous overhead lighting. All disks were weighed prior to testing to determine amount of repellent in treated textiles. Room temperature and relative humidity were recorded with a ThermoPro TP49 digital meter at the time of tests. Results are presented as mean (±SE) percent of mosquitoes ≥50% from repellent source.

4. Results and Discussion – Electrospun Fibers from recycled PET with Long-Term Insect Repellent Release

In this section, we demonstrate the use of recycled PET (rPET) from consumer drink bottles as a polymer feedstock for functional long-term insect repellent release from nonwoven microfiber mats. Fiber morphology and size were identified by SEM. Repellent retention in the electrospun fibers were tested using TGA. Release kinetics of the repellents from the fibers was calculated based on isothermal TGA experiments. We present the use of a novel live mosquito bioassay to evaluate the repellency of the electrospun PET fibers for 3 weeks. Repellency was observed in all fibers tested with the highest repellency observed at 100% for over one week. Our method provides DEET-loaded PET microfibers that exhibit extended mosquito repellency that significantly outperforms current commercially available repellent products.

4.1. rPET fiber motivation

In recent years, there has been an increase in insect-borne diseases. Topically applied insect repellents are used to prevent these infectious diseases, but concerns of skin permeability have given way to alternative delivery methods. Encapsulation of insect repellents in fibrous material allows for non-contact method of delivery of repellent with an extended-release profile without reapplication. PET is widely used in food packaging and is a major environmental pollutant, thus recycling PET is of great interest and utility. We report on the fabrication and evaluation of recycled PET microfibers containing DEET, picaridin, and a mixture of DEET/picaridin via electrospinning. The synthesized monofilament microfibers were shown to have the repellents within the polymer network with repellent retention up to 97%. Release profiles were characterized using isothermal TGA with a calculated repellent release half-life up to 23 days at room

temperature. Repellent chemical affinity was also evaluated using HSPs. Insect repellency was assessed against live mosquitos using a novel bioassy method. Repellency was observed to be as high as 100% for over 1 week and 80% at over 3 weeks. Our method allows for long-lasting repellency and the possibility of large-scale textile manufacturing.

4.2. rPET fiber morphology

Table 1. List of rPET sample abbreviations

Abbreviation	Definition
rPET	10 wt% recycled PET microfibers
rPET-10-D	rPET with 10 wt% DEET
rPET-30-D	rPET with 30 wt% DEET
rPET-50-D	rPET with 50 wt% DEET
rPET-60-D	rPET with 60 wt% DEET
rPET-70-D	rPET with 70 wt% DEET
rPET-40-P	rPET with 40 wt% Picaridin
rPET-50-P	rPET with 50 wt% Picaridin
rPET-15-DP	rPET with 15 wt% of 1:1 DEET/Picaridin
rPET-40-DP	rPET with 40 wt% of 1:1 DEET/Picaridin
rPET-54-DP	rPET with 54 wt% of 1:1 DEET/Picaridin

Electrospun microfibers at 10 wt% rPET loaded with 10-70 wt% repellents were synthesized using method discussed above in Section 3, Materials & Methods. Repellents used were DEET, picaridin, and a 1:1 mixture of DEET and picaridin. The effects of repellent concentration relative to the PET on fiber diameter and morphology were evaluated with SEM. Fiber diameter varied greatly for all fibers synthesized as seen in Figure 5. Our previous studies with repellent loaded nylon fibers produced nanofibers (100 – 500 nm)[23-24], while rPET allowed for microfibers (0.6 – 4.0 μm) to be obtained. Fiber morphology was dependent on insect repellent type, combination, and retention. Common morphologies observed were cylindrical, ribbon-like, beading, branching, and loops. Cylindrical shape is normal morphology for fibers. Ribbon-like shape occurs when fiber diameter reaches its capacity and the structure collapses on itself[53]. The

imbalance of surface tension and electrical forces can also affect the shape of the fiber. This instability results in the ejecting of a smaller fiber from the primary fiber in what is called branching. This splitting can also result in loops where the smaller branched fibers spin upon themselves forming a larger segmented fiber. When the electrical forces are reduced the surface tension forces fluid into the beads[54]. Recycled PET fibers containing no repellents were cylindrical and free from defects, Figure 2. DEET fibers contained a mixture of morphologies. Both cylindrical and ribbon fibers occurred in all DEET-loaded fibers tested. Morphological defects increased with increasing DEET loading. Branches and loops were prevalent in fibers containing 50 and 60 wt% DEET. Beading as well as branching occurs in 70 wt% DEET fibers. Picaridin fibers contained ribbon-like morphology with some branching. Fibers containing a blend of repellents had ribbon-like and cylindrical fibers at 15 wt% with branching. When repellent loading increased to 40 and 54 wt% only the ribbon-like morphology was observed.

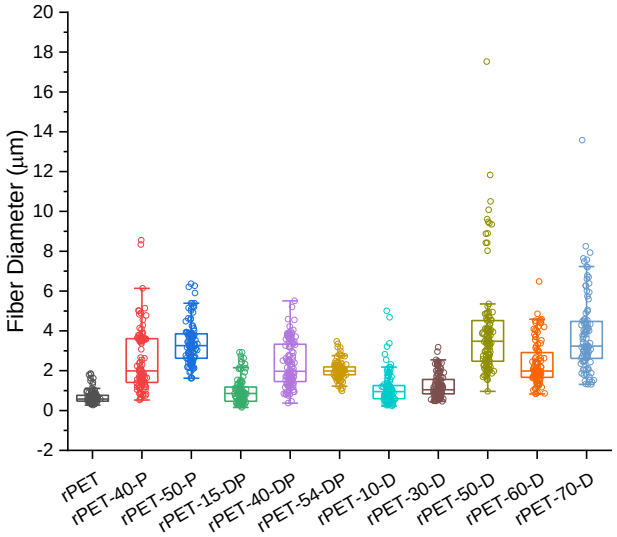

Figure 5. Fiber diameters of monofilament rPET fibers in a box plot where dots represent the individual measurements.

The amount of insect repellent retained in the electrospun fibers was determined using TGA. Fibers were subjected to increasing temperature from room temperature to 600 °C at 10

°C/min to evaluate the mass loss within the ramp, Figure 6E-F. The decrease in fiber mass at 250 °C was attributed to loss of insect repellent, from which the percentage of repellent retained was calculated[23]. After electrospinning, DEET rPET fibers retained 80.0-97.5% of DEET from the initial electrospinning solution, Table 2. Picaridin rPET fibers retained nearly all (97.5%) after electrospinning. The greater retention of picaridin than DEET in rPET electrospun fibers was attributed to the lower vapor pressure of picaridin. Repellent retention in DEET/picaridin rPET fibers ranged from 54.1% to 87.2%. The use of dual-repellents causes an increase of evaporation during electrospinning. Headspace analysis was performed using GC/MS to determine analytes present during evaporation at room temperature.

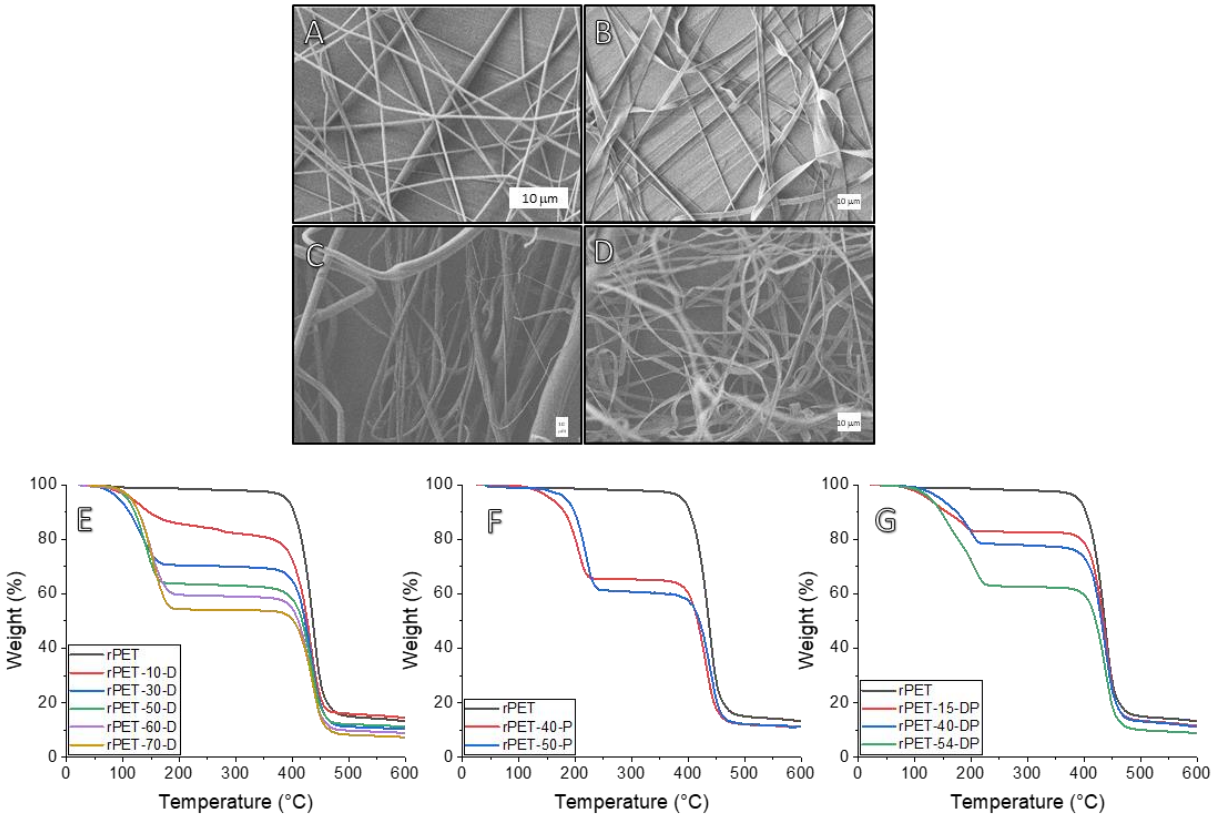

Figure 6. Scanning electron microscope (SEM) images of electrospun rPET microfibers with (A) no repellent loading, (B) 50 wt% Picaridin, (C) 50 wt% DEET (D) 54 wt% DEET/Picaridin. Thermogravimetric analysis (TGA) heating ramps showing the mass loss of repellent from fibers containing (E) 0 – 70 wt% DEET (F) 0 – 50 wt% picaridin and (G) 0 – 54 wt% DEET/Picaridin blend

Headspace analysis was performed on rPET-54-DP fibers to identify the relative rates of release. The headspace of a neat DEET and picaridin blend was first evaluated as a standard to identify the GC peaks that correspond to each repellent. DEET and 2-butanol were preliminarily identified from the DEET/picaridin standard mixture, in addition to siloxane containing compounds attributed to column decay. 2-Butanol is a known fragment of picaridin[55] and the most abundant in the headspace. The headspace of rPET-54-DP was tested at 2 h, 1, and 7 days. Again, 2-butanol and DEET were two major compounds within the headspace throughout the study. Significantly, trifluoroacetic acid and DCM were not identified in the headspace, thus indicating no residual solvent in the rPET-54-DP fibers.

Table 2. Repellent retention of rPET electrospun microfibers.

Sample	**Retention (wt%)**
rPET	-
rPET-10-D	80.0
rPET-30-D	97.5
rPET-50-D	88.0
rPET-60-D	89.1
rPET-70-D	94.0
rPET-40-P	97.5
rPET-50-P	97.6
rPET-15-DP	79.7
rPET-40-DP	54.1
rPET-54-DP	87.2

ATR-FTIR was used to determine the composition of the rPET fibers. Fibers from

solutions containing rPET with 0 wt% repellent, 50 wt% DEET, 50 wt% picaridin and 54 wt% DEET/picaridin were evaluated using ATR-FTIR (Figure 7). The characteristic bands of PET occurred in all fibers at 2978 and 2852 cm $^{-1}$ (C-H stretching), 1715 cm^{-1} (C=O stretching of carboxylic ester group), 1581, 1506, and 1409 cm^{-1} (C=C aromatic stretching), 1453 and 870 cm^{-1} (CH_2 bending and rocking), sharp peaks at 1238 and 1090 cm^{-1} (C-C-O stretching of ester group), sharp peaks at 1015 and 723 cm^{-1} (in-plane C-H stretching and out-of-plane C-H bending of aromatic ring)[56]. In the insect repellent loaded fibers, peaks corresponding to repellents were observed and confirmed incorporation of IRs, however most peaks associated with the repellents overlap with rPET peaks due to the structural similarities. Notably, the sharp C=O stretch at 1626 cm^{-1} associated with DEET shifted slightly higher wavenumber to 1630 cm^{-1} in rPET-50-D fibers suggesting potential intermolecular interactions between rPET and DEET, similar to behavior previously observed in PLLA-DEET fibers[26]. This behavior is also observed in rPET-50-P fibers, the sharp peak at 1659 cm^{-1} from the hydrogen bonded carbamate carbonyl (C=O) stretch associated with picaridin shifted to 1670 cm^{-1}. Additionally, lack of shifts in the repellent peaks in rPET fibers suggests physical entrapment of repellent within the polymer matrix.

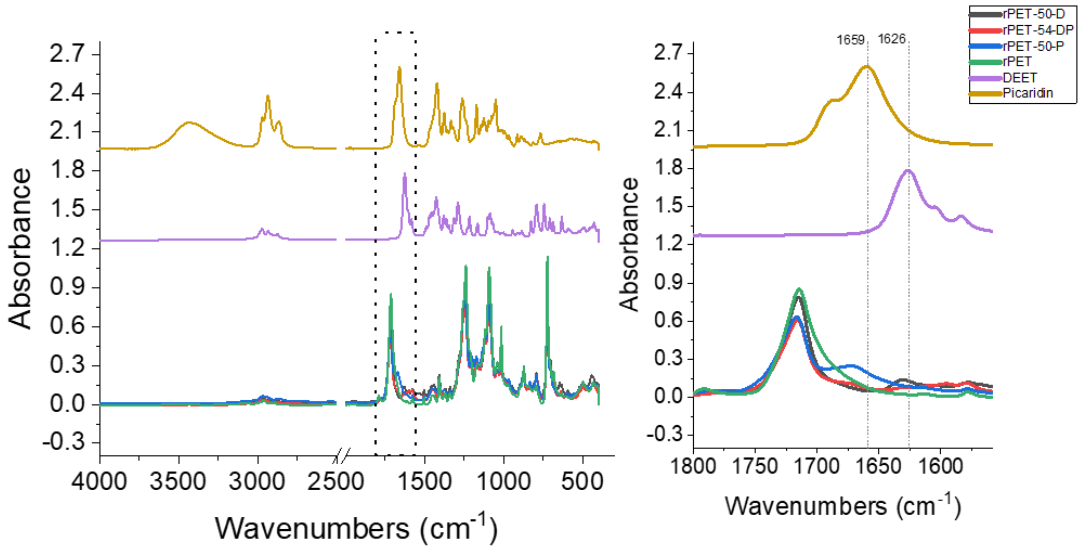

Figure 7. ATR-FTIR of electrospun microfibers from electrospun microfibers rPET, rPET-50-D, rPET-50-P, rPET-54-DP, neat DEET and picaridin composites showing the full spectrum (left) and the area of interest (right).

4.3. Insect repellent release kinetics

Measuring repellent release rate kinetics and calculations of repellent lifetime is an important factor to elucidate to understand compositional effects on release and predict future repellent performance. Isothermal TGA experiments were conducted at 60, 80, and 100 °C to determine the release rate of repellents. Each experiment was maintained for 5 h where the mass loss over time was attributed to the evaporation of repellent. The data was fit to a first order reaction model (Equation 1) to calculate the rate constant (k) at each temperature. Where y is the mass percent remaining of the sample for a given temperature at time, t. A is defined as a pre-exponential factor, k, is the rate constant in s^{-1}, and c is a constant for fitting purposes.

$$y = A \text{ x } e^{-kt} + c \quad (1)$$

The rate constant was then used to calculate the activation energy (Ea) using the linearized Arrhenius equation (Equation 2). Where k is the calculated rate constant, R, is the universal gas constant (8.314 J/mol·K), and T is the temperature in Kelvin. The ln(k) was plotted against their

given temperatures and the generated slope was used to calculate the activation energy.

$$\ln(k) = \frac{-E_a}{R}\left(\frac{1}{T}\right) + \ln(A) \quad (2)$$

The half-life was also calculated at using Equation (3).

$$T_{1/2} = 0.693/k \quad (3)$$

The release profiles of rPET-50-D, rPET-50-P, and rPET-55-DP were evaluated in this study. Figure 8 displays the profile of 54 wt% DEET/picaridin 1:1 blend, the profiles of the remaining fibers can be found in the supplemental information. Expectedly, the rate at which repellent evaporates increases with increasing temperature (Figure 8A). A plot of the ln(*k*) vs. the inverse temperatures (Figure 8B) gave a linear fit line which was used to calculate E_a using Equation 2. From this, the rate constant at for hypothetical 20 °C was calculated and was used in Equation 3 to determine the half-life of each sample at room temperature. Identifying fiber performance at 20 °C was imperative due to high mosquito activity at ambient temperatures[57]. Activation energy, rate constant and half-life of samples tested are displayed in Table 3.

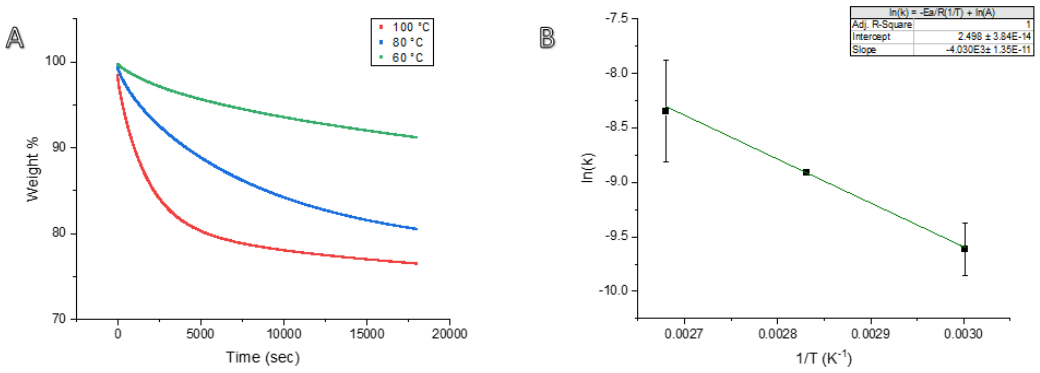

Figure 8. (A) Isothermal release profile of rPET with 54 wt% DEET/picaridin microfibers at 60, 80, 100 °C. (B) Linear fit for the Arrhenius analysis used to determine the activation energy of rPET with 54 wt% DEET/picaridin electrospun microfibers. Error bars are a result of triplicate measure.

Table 3. Activation energy, rate constant, and half-life of repellents at 20 °C from electrospun microfibers. Errors indicate a triplicate measurement.

Repellent	***E_a (kJ/mol)***	***k* (s^{-1}), at 20 °C**	***$t_{1/2}$* (h), at 20 °C**
rPET-50-D	85.4 ± 17.6	$3.53 \times 10^{-7} \pm 1.03 \times 10^{-6}$	545.8 ± 160
rPET-50-P	17.4 ± 5.5	$3.31 \times 10^{-5} \pm 1.12 \times 10^{-4}$	5.82 ± 1.7
rPET-55-DP	33.5 ± 10.7	$1.30 \times 10^{-5} \pm 2.74 \times 10^{-5}$	14.8 ± 7.0

The activity of each repellent differed greatly. The rate constant for the loss of repellent at 20 °C ranged from 3.53×10^{-7} to 1.3×10^{-5} s^{-1} with picaridin having the highest and DEET having the lowest rate of release. This also translated to activation energy and half-life. Picaridin rPET fibers exhibited a half-life comparable to picaridin spray, suggesting minimal intermolecular interaction between picaridin and rPET. While the DEET/picaridin rPET fibers resulted in an increased activation energy (33.5 kJ/mol) and half-life (14.8 h). DEET rPET fibers were calculated to have an activation energy of 85.4 kJ/mol and a significantly long half-life of 545.8 h (22.7 days). This is a significant increase in half-life compared to the previous study of DEET loaded nylon 6,6 fibers[23], indicating potential positive intermolecular interactions between DEET and rPET to effectively slow the release of DEET. The calculated release kinetics of the fibers were compared to actual performance using live insect testing.

4.4. Live-insect bioassay

Fibrous rPET mats were subjected to a novel bioassay to evaluate their efficacy for live mosquito repellency over multiple weeks. This bioassay was specifically designed to evaluate the long-term repellent efficacy of insect repellent-loaded fibers and textiles, and this represents the first report of the use of this bioassay in the evaluation of insect repellent-loaded materials. rPET nonwoven mats were first evaluated over a 24 h span during continuous exposure to identify the

role of insect repellent composition on repellency and validate the bioassay method. Separate mosquito populations were exposed to rPET, rPET-50-D, rPET-50-P, and rPET-54-DP nonwoven mats. Furthermore, this study aimed to identify possible synergistic effects from the combination of DEET and picaridin in the same fibers system. Figure 9 presents the results of the 24 h study, where the percent repellency was determined as the percentage of mosquitoes on the opposite half of the test tube. It is expected that if a material exhibited no repellent effect, then the mosquitos would be uniformly distributed throughout the tube thus resulting in a value of 50% mosquitos repelled, as probability dictates at any time half of the mosquitos would be in one half of the tube. Expectedly, the rPET exhibited an average repellency of 39.5±7.2%, which clearly represents no repellency in the unmodified fiber. Incorporation of picaridin in rPET fibers resulted in only minor improvement over the control at some time points, but was mostly statistically similar to the control. Both rPET-50-D and rPET-54-DP fibers demonstrated very high repellency immediately within 90% range and both maintained approximately 100% repellency through 24 h. Commercial insect repellent sprays exhibit repellency on the order of several hours[13]. Since both rPET-50-D and rPET-54-DP fibers exhibited near 100% repellency over the full 24 h, potential synergistic effects were not able to be resolved from this study. Further evaluation of the fibers was performed to identify the entire duration of effective repellency of the insect repellent loaded rPET fibers.

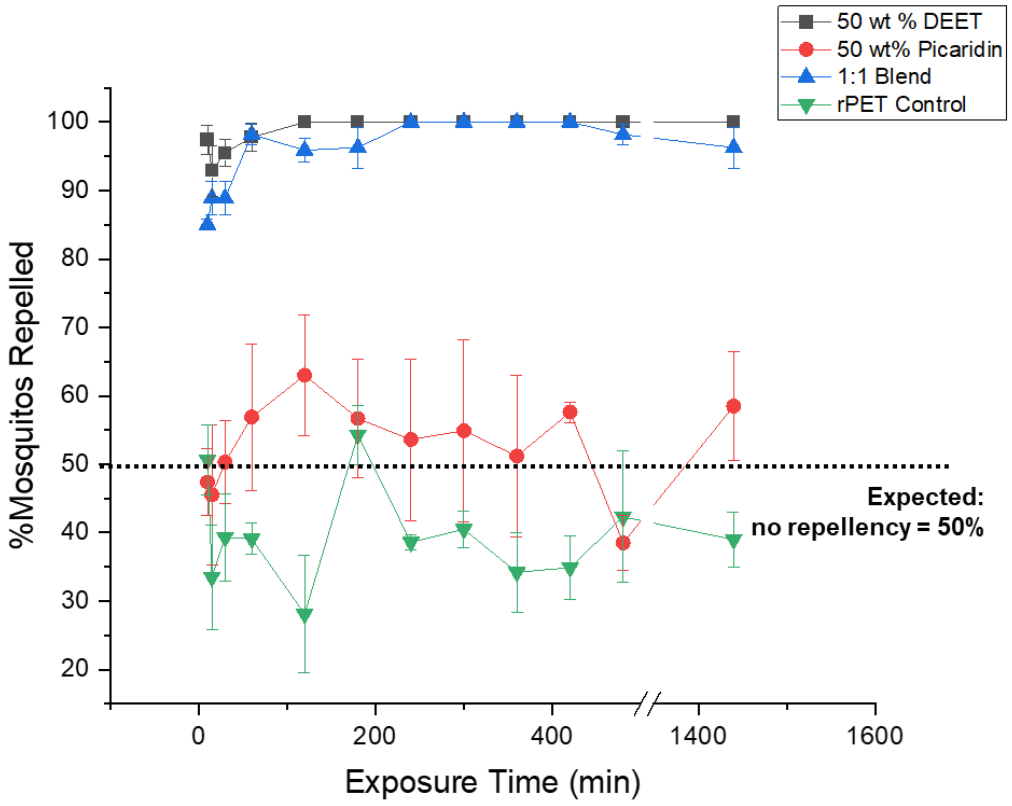

Figure 9. Live insect testing of rPET, rPET-50-P, rPET-50-D and rPET-54-DP electrospun nonwoven microfiber mats over 24 h.

A three-week study was conducted on the rPET fibers to determine the effects of long-term aging on repellent performance. Over the course of 3 weeks, the fibers were tested for 8 h at each set time (0 h, 24 h, 1 week, 2 weeks, and 3 weeks). The fibers resided at room temperature in open air between time sets for the entire 3-week duration. The performance of rPET, rPET-50-P, rPET-50-D, rPET-54-DP, and a blank metal screen are detailed in Figure 10. The blank metal screen was incorporated as a negative control to confirm the behavior of the mosquitoes and further validate the test method. The range of the screen repellency was approximately 50% for the entire 3-week duration, which serves as a negative control to validate that the test method does not bias for repellency or non-repellency. The rPET control also demonstrated close to 50% repellency over 3 weeks, similar to that of the screen alone, indicating that the unmodified rPET does not exhibit

any insect repellent effect. The initial repellency of rPET-50-P was approx. 40% and the repellency increased to approx. 85% at 5 h, suggesting potential slow release of picaridin from the rPET fiber matrix. The rPET-50-D fibers exhibited 100% repellency through 32 h and at 1 week remained at approximately 80%. At 3 weeks, rPET-50-D fibers still exhibited some repellency of 60-70%, which was greater than that of the controls, however by 3 weeks the variability of rPET-50-D increased significantly. The rPET-54-DP fibers demonstrated long-term repellent efficacy over 2-3 weeks, with nearly 100% repellency over the first 32 h. Significantly, rPET-54-DP fibers maintained an approximate 90% repellency through weeks 1 and 2, representing long-term repellency, and rPET-54-DP fibers repellency was still within the 80% range at 3 weeks. Although the role of synergistic effects on repellent efficacy are unclear, repellency variability decreased in fibers containing both repellents. Notably, there is a benefit to dual repellent loading in the polymer matrix.

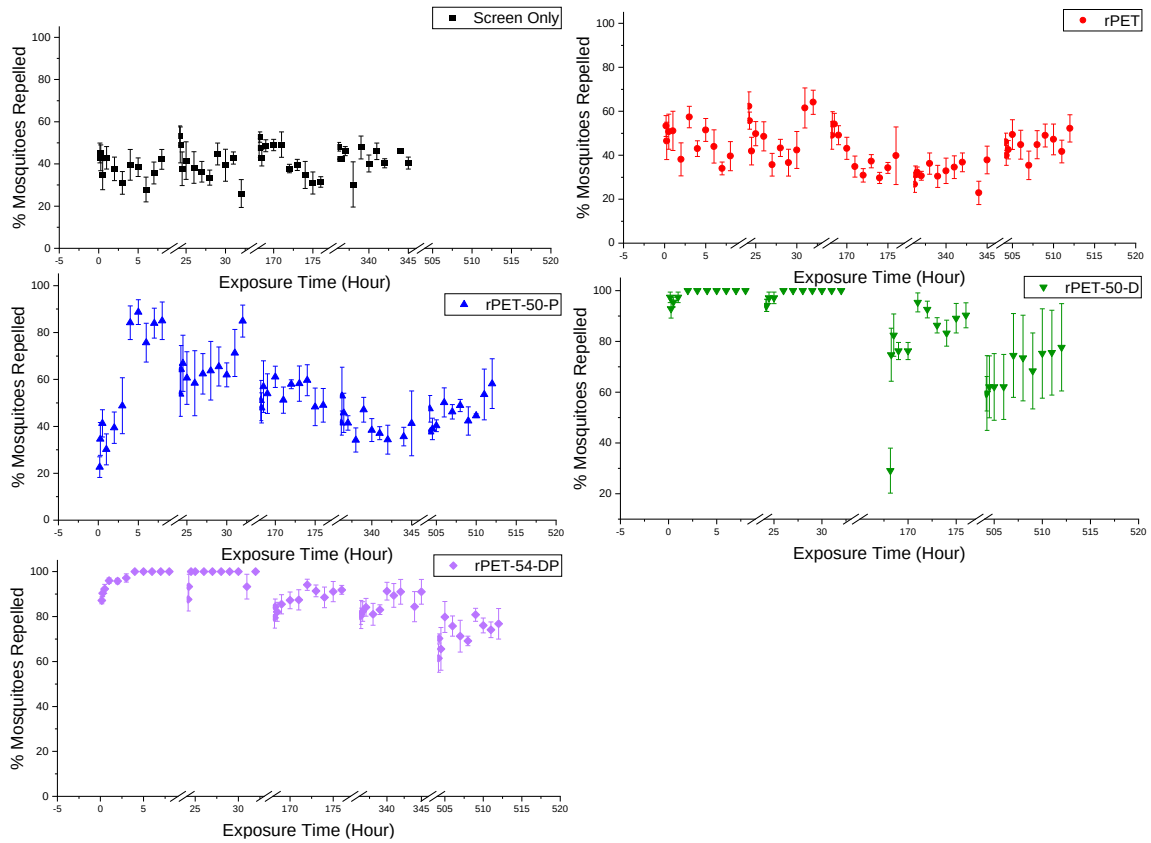

Figure 10. Live insect testing of rPET, rPET-50-P, rPET-50-D and rPET-54-DP electrospun nonwoven microfiber mats. The study was conducted for 3 weeks with testing at 0 h, 24 h, 1 week, 2 weeks, and 3 weeks. An 8 h evaluation was conducted at each testing time with repellency observations at 10 min, 15 min, 30 min, 1 h, 2 h, 3 h, 4 h, 5 h, 5 h, 6 h, 7 h, and 8 h. Error bars represent n>3.

4.5. Proposed Physical Model

Hansen Solubility Parameters (HSPs) have demonstrated quantified relationships on the issue of solubility, dispersion, diffusion and more through its direct correlation with chemical affinity. Hansen solubility parameters are a tri-component position where δ_d, δ_p, and δ_h are the dispersion, polar, and hydrogen bonding parameters, respectively. As the distance between two coordinates (R_a) in "Hansen space" decreases, the chemical affinity between those two chemicals or mixtures increases. Polymers exhibit an inherent interaction radius (R_o) wherein solvents or solvent mixtures within or on this radius ($Ra/Ro \leq 1$) will dissolve or swell the polymer. If Ra/R_o

> 1, the solvent or solvent mixture will exhibit no chemical affinity to the polymer. This Ra/R_o ratio is also called the Relative Energy Difference (RED) value.

The RED PET values show DEET, picaridin and DEET/Picaridin blend exhibiting a RED PET value <1 compared to the RED nylon 6,6 values ≥1. This indicates a higher chemical affinity between PET and the insect repellents as all reside within the inherent interaction radius in Hansen space (Figure 11). The 1:1 DEET/picaridin exhibits a lower RED PET value than the individual insect repellents alone. This higher chemical affinity can aid in the retention of insect repellents within the polymer matrix therefor resulting in the distinctly longer repellency in live mosquito testing as observed in the 1:1 DEET/Picaridin fibers. This also further explains the results of previous studies of electrospun nylon 6,6 loaded with DEET in which DEET-Nylon fibers exhibited a shorter half-life relative to DEET-PET fibers. The RED value for nylon and DEET indicated no chemical affinity between polymer and insect repellent as DEET resides outside of the inherent interaction radius in Hansen space (Figure 11).

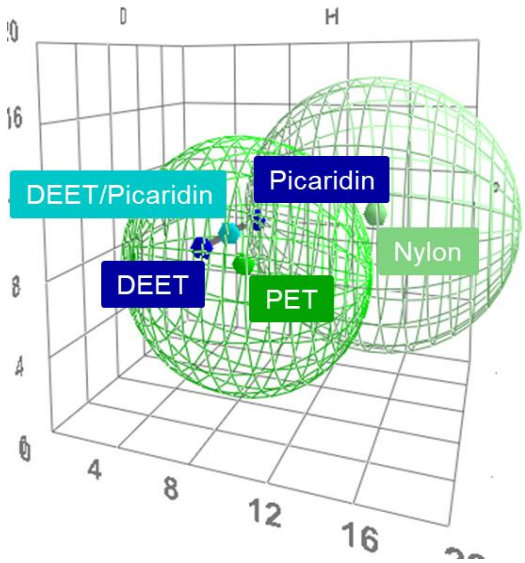

Figure 11. Calculated HSP plot. Left sphere is of PET and right sphere is of nylon. The blue dots represent DEET, DEET/Picaridin and picaridin. Repellents are within the sphere of PET indicating good affinity to the polymer.

Based on the HSP analysis and IR analysis, we propose a physical interpretation of the insect repellent loading in PET and the molecular interactions dictating release behavior. Strong intermolecular interaction between DEET-PET resulting from the polar interactions from the carbonyl, amide, and ester, as well as pi-pi interactions of aromatic rings in each compound are responsible for the high retention of DEET and the extended-release profile. In fibers containing DEET, the combination of polar-polar and aromatic interactions facilitated the dispersion of DEET throughout the PET matrix. Furthermore, the polar and pi- intermolecular interactions contributed an energetic barrier, over which the DEET had to overcome to volatilize, resulting in extended-release profiles and long-term repellent release. In picaridin-PET fibers, the polar contributions were weaker and the aromatic component absent, thus the release of picaridin-PET was not significantly improved compared to neat picaridin. The dual-repellent-loaded fibers demonstrated additive behavior of the independent DEET and picaridin interactions, thus resulting in an intermediate release profile where the improvement was attributed to DEET-PET interactions. Ultimately, the live insect release behavior was primarily dependent on the amount of repellent that remained in the PET fibers at any given time, and therefore the intermolecular interactions between the repellent and polymer matrix, as predicted with HSPs, represent and effective approach to design and modulate the release profile and live insect release performance in IR-loaded polymer fibers.

4.6. rPET Fibers: Conclusions

Microfibers composed of recycled PET consumer bottles and EPA-registered insect repellents were fabricated via electrospinning. Characterization of the fibers indicated entrapment to the repellents within the polymer that allows for the extended release of the repellent via

diffusion. Morphology and fiber thickness varied throughout all fibers, however, it did not interfere with the retention of repellents after electrospinning with retention rates up to 97%. Repellent rate constants and half-life was calculates using isothermal TGA experiments at room temperature. It was shown that rPET fibers with 50 wt% DEET exhibit significantly long release times with a half-life nearly 23 days. Nonwoven mats containing repellents were tested against live mosquitoes initially over a 24 h period where 100% repellency was observed with 50 wt% DEET and 54 wt% DEET/picaridin fibers. Further study on the performance of the fibers as they aged was conducted. Further, 50 wt% DEET and 54 wt% DEET/picaridin fibers continued to repel above the controlled environments throughout the 3-week study. The repellent blend showed higher performance with precision of repellency. Investigation of the solvent interactions of repellents and polymer strongly correlate the performance with the chemical affinity. The repellent blend was calculated to have highest chemical affinity to rPET allowing for extended diffusion of the repellents thus longer repellency. Commercially available repellent sprays can maintain their repellency up to 10 h for DEET and 8 h for picaridin before reapplication[58]. Our method allows for repellency beyond 3 weeks as the study indicates continued repellency of 80% at 3 weeks for fibers containing 1:1 DEET/picaridin blend. As such, the IR loaded-PET fibers described herein represented a novel fiber-based long-term insect repellent platform for potential patch, yarn feedstock, or textile applications (Figure 12). Future work will focus on the durability of the fibers through laundering, as well as transition to the extrusion of fibers for manufacturing of textiles and fabrics.

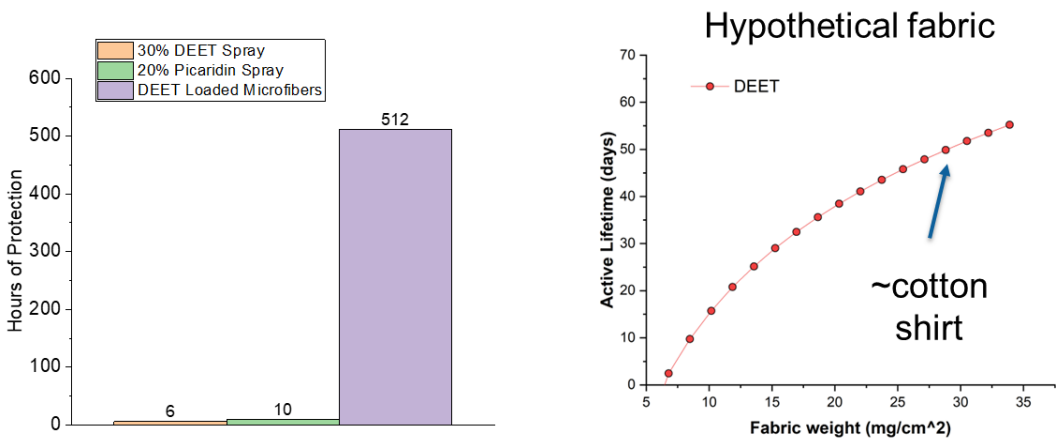

Figure 12. Comparison of efficacy lifetime between commercial DEET- and picaridin-based sprays to rPET-50-D (left). Calculated expected repellent lifetime of a hypothetical fabrics composed of rPET-50-D as a function of fabric weight (right).

5. Results and Discussion – Modacrylic DEET Gels

In this section, we report on the design of physical gels centered around DEET, the most common EPA-registered active ingredient in insect repellents, as the gelling solvent for compatibility with dry jet wet spinning (Figure 13). Common textile filaments were analyzed for their miscibility with DEET through HSPs to be repurposed as insect repelling physical gels thus inducing a circular economy. Insect repellency will be determined through diffusion analysis and live insect testing.

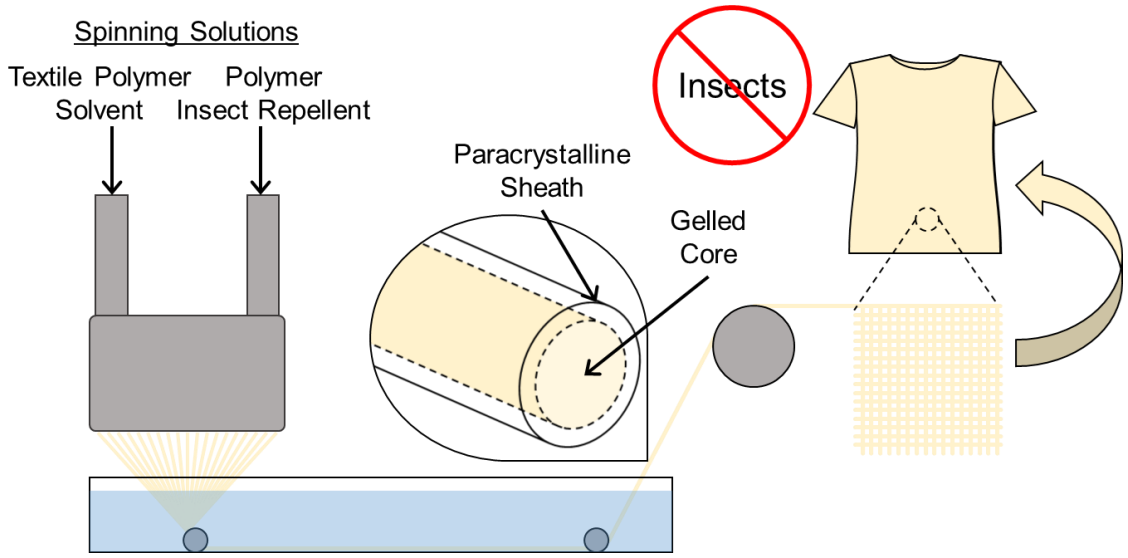

Figure 13. Conceptualization of dry jet wet spinning to fabricate insect repellent bicomponent fibers and application to produce textiles.

5.1. Motivation and Concept

This physical gel will ultimately be purposed in a bicomponent fiber design (Figure 14) where a paracrystalline sheath provides protective barrier and apparel-grade mechanical properties while the physically gelled core serves as a reservoir for high loading of insect repellents to facilitate long-term release. To achieve the design as proposed in Figure 14, we have established four objectives. First, identify a core polymer solution suitable for gelation with insect repellents.

Second, identify a sheath polymer suitable for textile applications while maintaining high barrier properties. Third, optimize spinning solutions for dry-jet gel spinning. And fourth, analyze resulting samples.

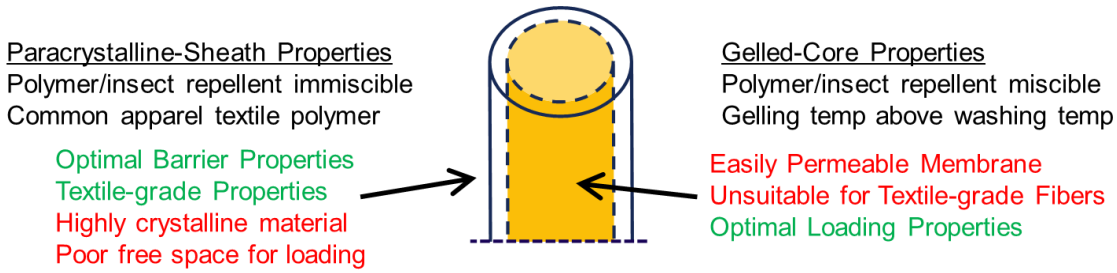

Figure 14. Bicomponent paracrystalline-sheath with gelled-core fiber design.

5.2. Core Polymer Identification

DEET has shown to be within the inherent interaction radius of an array of polymers as correlated with a RED ≤ 1 which indicates that DEET is miscible with the polymer (Figure 15A). Polyvinyl chloride is a thermoplastic polymer with a degradation temperature lower than its melting temperature, thus being an important polymer in fire retardant textiles. Specifically, modacrylic copolymers of acrylonitrile and vinyl chloride are commercially produced for various fire-retardant applications such as children's garments, upholstery, faux fur, and protective outerwear. Therefore, we aimed to repurpose this largely produced and available copolymer type for physical gels.

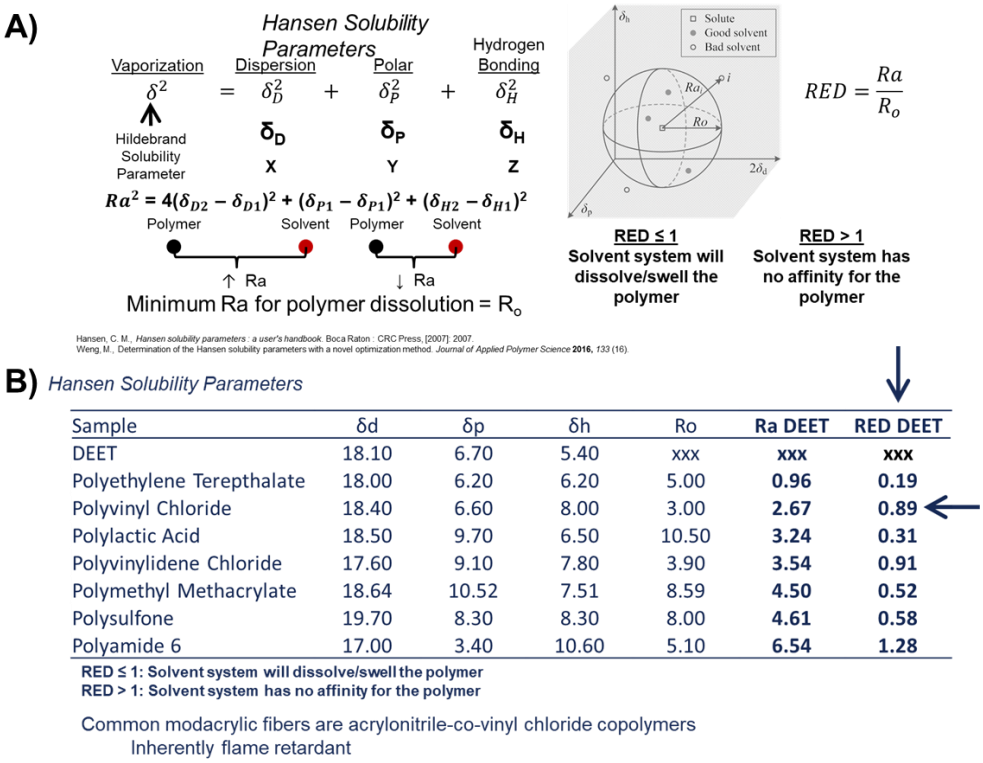

Figure 15. A) Application of Hansen Solubility Parameters (HSPs) to determine RED values. B) Application of HSPs to identify textile polymers compatible with DEET for gelled core.

Modacrylic filaments composed of 1:1 mol/mol acrylonitrile-co-vinyl chloride (P(AN-VC)) had an RED value of 0.90 to DEET, suggesting miscibility (Figure 16). Upon bulk fiber dissolution in DEET at 130 °C, P(AN-VC)/DEET systems were achieved at varying concentrations. For optimal washfastness properties, the gel temperature should exceed laundering temperatures to retain the gelled morphology. AATCC 61-1A standard conducts washfastness testing at 40 °C which correlates to the "warm" setting on commercial washing machines; therefore, a target gel temperature of 45 °C was selected.

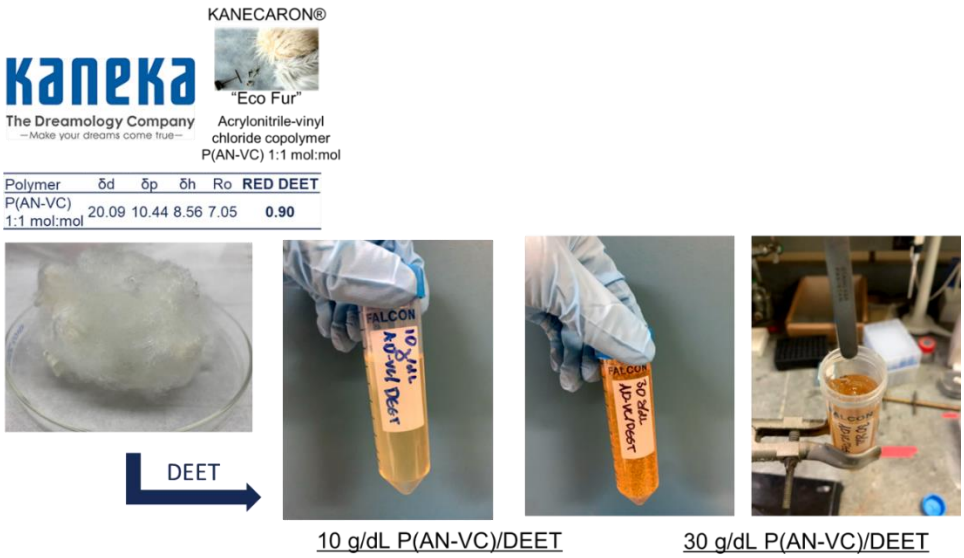

Figure 16. Demonstration of gelled P(AN-VC) with DEET at 10 g/dL and 30 g/dL.

Rheological temperature sweeps at a frequency of 1 Hz were conducted at varying polymer concentrations to determine the gelation temperature (Figure 17). A linear correlation between gel temperature and polymer concentration was found for P(AN-VC)/DEET systems as seen in Figure 17-2. Utilizing this trend line, an accurate extrapolation determined that a gel temperature of 45 °C is achieved with a P(AN-VC)/DEET concentration of 47.5 g/dL (Figure 17-3). The resulting system at room temperature possessed hard gel physical properties.

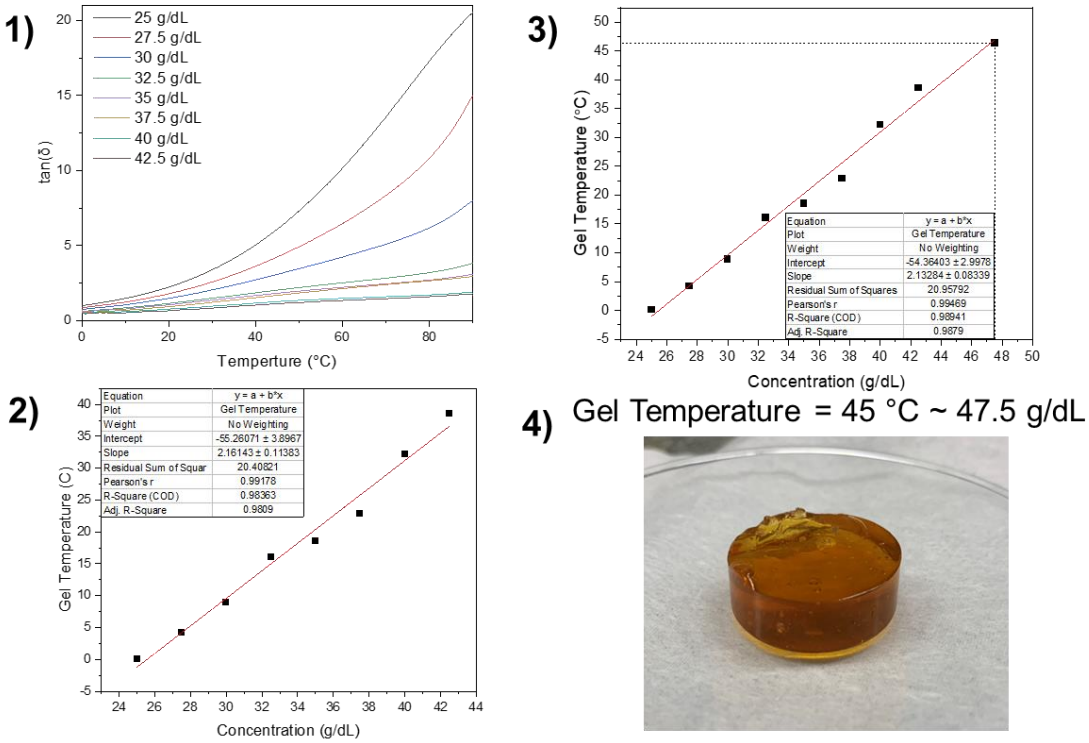

Figure 17. 1) Rheological analysis of P(AN-VC)/DEET solutions of increasing concentration as a function of temperature. 2) Gel temperature determined from rheology as a function of P(AN-VC)/DEET concentration and observed linear relationship. 3) Extrapolation of linear fit to target gel temperature (45 °C) and accurate prediction of gel temperature at 47.5 g/dL (black square). 4) Representative image of 47.5 g/dL P(AN-VC)/DEET gel demonstrating transparent, amber appearance.

5.3. Sheath Polymer Identification

To maintain optimal barrier and mechanical properties within the sheath, the sheath polymer should be immiscible with DEET to slow diffusion through the membrane and also prevent crystallite disruption within the polymer matrix. HSPs in Figure 18 showed potential sheath candidates with RED DEET > 1 values which indicate immiscibility. Cellulose acetate was chosen for its immiscibility in conjunction with its flame-retardant properties.

Polymer	Dissolving Solvent	RED DEET	Melting Temperature (°C)
Cellulose	NMMO; DMAc/LiCl	1.25	N/A
Wool	N/A	N/A	N/A
PET	TFA/DCM	0.19	250
→ Cellulose Acetate	Acetic Acid; Acetone	1.06	N/A
PAN	DMSO; DMF; DMAc	1.01	N/A

RED ≤ 1: Solvent system will dissolve/swell the polymer
RED > 1: Solvent system has no affinity for the polymer

Figure 18. Application of HSP theory to identify promising paracrystalline sheath polymer (cellulose acetate).

5.4. Optimization of Spinning Solutions

Spinnability utilizing dry-jet wet spinning techniques has been rheologically correlated with a zero-shear viscosity between 20-30 kPa·s, as calculated by the cross model.[59] Frequency sweeps of 47.5 g/dL P(AN-VC) at different temperatures were conducted to extrapolate the zero shear viscosity (Figure 19A). An Arrhenius equation was used to fit the zero-shear viscosity with temperature and accurately used to extrapolate a temperature of ~76 °C to be within the target range.

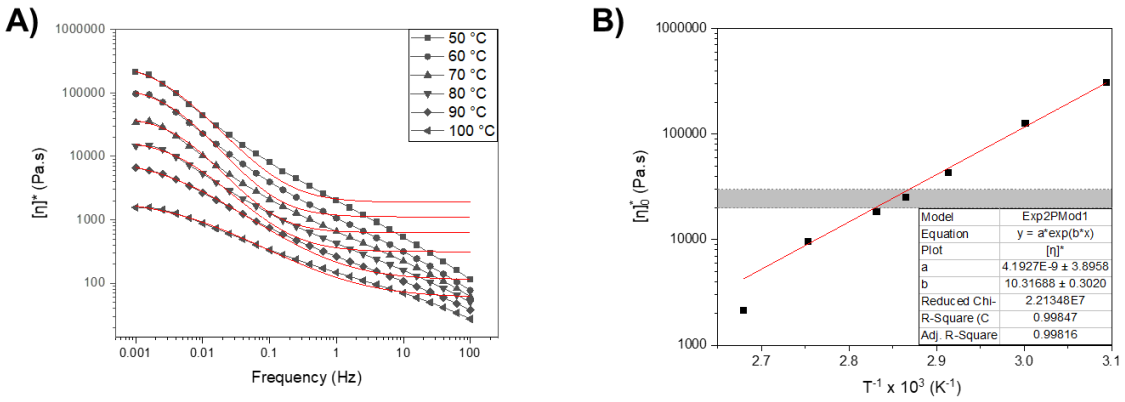

Figure 19. A) Cross model fit to determine zero-shear viscosity. B) Fitted using Arrhenius's equation, 30 kPa·s zero-shear viscosity = ~76 °C

5.5. Preliminary proof of concept

Preliminary gel spinning of 47.5 g/dL P(AN-VC)/DEET was successfully performed through a simple syringe and take-up system (Figure 20). The applied temperature on the syringe

was 160 °C; however, the temperature of the P(AN-VC)/DEET "semi-molten" upon exiting the capillary was ~75 °C. Therefore, appropriate measures to insulate the heated syringe system will be investigated. A feed rate of 0.3 mL/min and take-up of 110 m/min successfully resulted in gelled filaments. The resulting filaments exhibited low tensile strength and high elongation due to the gelled morphology. Subsequent initiatives will look towards designing a sheath spinning solution to implement protective barrier properties and apparel-grade mechanical properties while also achieving similar rheological properties under these spinning parameters.

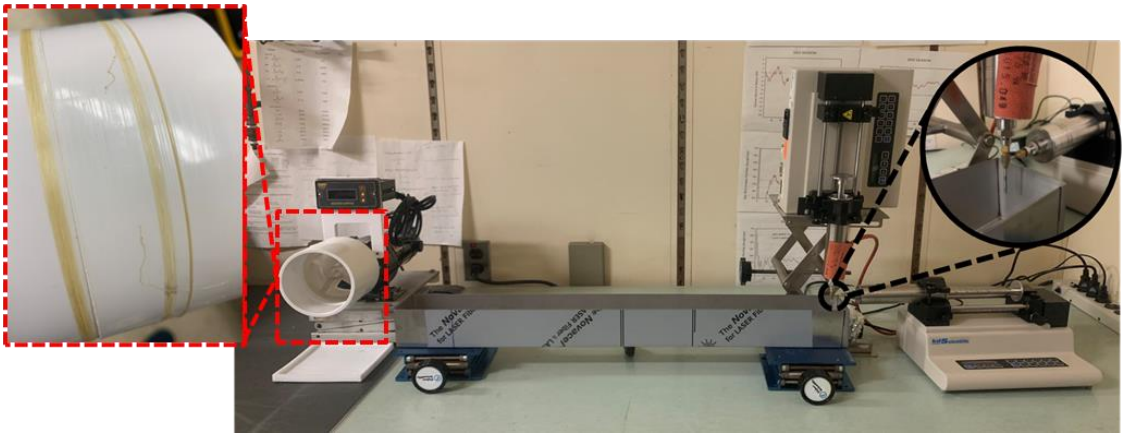

Figure 20. Lab-scale dry jet wet spinning apparatus capability of coaxial (bicomponent) fiber fabrication (right-inset) and demonstration of P(AN-VC)/DEET filaments collected onto the spool (left-inset).

5.6. Modacrylic Gels: Conclusions

Modacrylic physical gels highly-loaded with insect repellent were successfully designed through HSP theory. A 47.5 g/dL P(AN-VC)/DEET system possessed a gel temperature of 45 °C to maintain a gelled morphology during laundering under the "warm" setting. Moreover, spinning conditions to achieve dry-jet wet spinning was determined through rheological correlations. A sheath core composed of cellulose acetate with the potential of implementing other sheath polymer systems will be tuned for these spinning parameters.

6. Results and Discussion – Reducing Nylon Melt Extrusion Processing Temp.

One strategy to improve the insect repellency of textile fibers is to incorporate functional components into the fiber at the time of filament production or during the weaving step. An NRL-led SERDP effort is using electrospinning to incorporate insect repellents to screen a number of fiber and repellent compositions and morphologies. To support this effort, ARL has been evaluating the use of plasticizers to inhibit the crystallization of nylon matrix materials (e.g., nylon-11, -12). Using a small batch conical twin screw extruder, varying compositions of matrix and plasticizer were prepared and evaluated using thermal analysis techniques. Impacts on the peak crystalline melting temperature were determined, and a down-selected composition was prepared as a master-batch to enable subsequent low-temperature melt processing of the plasticized blend and a variety of insect repellents and insecticides.

6.1. Concept and Motivation

The incorporation of EPA-registered repellents, including DEET and picaridin, into textile-grade polymer filaments via melt extrusion is conventionally limited by the high processing temperatures. Additionally, flammability and flash point considerations of insect repellents become significant at elevated temperatures (e.g., > 200 °C). Nylon is a widely used polymer for textile applications that is produced commercially through melt extrusion at temperatures ca. 220 °C – 260 °C. Therefore, our objective was to reduce the melt temperature of nylon to enable improved retention of repellent and allow use of volatile repellents

6.2. Evaluation of Melt Depressants

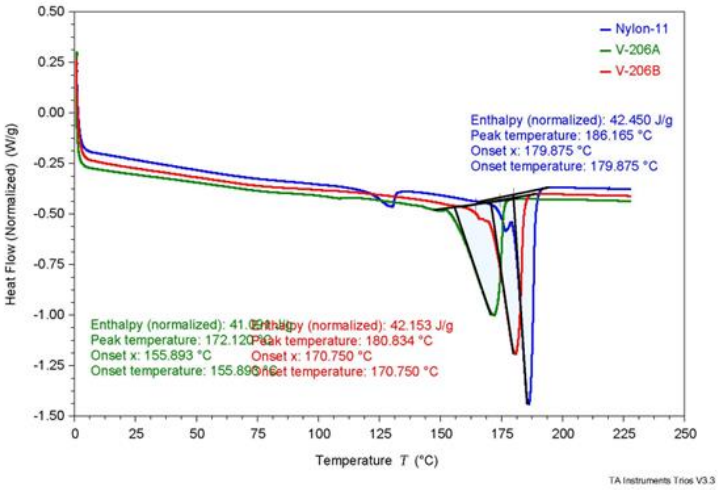

Figure 21. DSC thermogram demonstrating decreasing melting point of nylon-11 as a function of increasing pTSAm concentration.

Two plasticizers were initially selected for evaluation, one originating from literature references (*para*-toluenesulfonamide, pTSAm), and from the predicted compatibility of the plasticizer with both the amide matrix and the candidate repellents. Using HSPs, NRL identified evaluation of methylsulfonylmethane (MSM), which is also used commercially as a nutritional supplement. Testing protocols involved evaluation of batch mixes on ca 15 mL scale using a DSM Xplore Microcompounder to ensure good mixing of the constituents. The Xplore is a conical twin-screw extruder that uses a recirculation pathway to simulate a longer residence time or l/d ratio. Loading levels of 20 and 30 wt/wt were probed, along with a single-stage dilution at of each composition, resulting in a ca. 66% reduction of loading for the diluted batch. Impacts on matrix characteristics were assessed using dynamic scanning calorimetry (DSC). Nylon-11 was used as the matrix for the initial screening of plasticizers.

The pTSAm plasticizer was found to form a good alloy with the nylon-11, resulting in a single melting transition and significant reduction in the melting peak. The MSM plasticizer was also effective in reducing the melting peak temperature for the blends, but appeared to perhaps be

less soluble with the matrix. A distinct melting peak for MSM was still observed when looking at the blend characteristics. A summary of observed plasticizer and composition correlated with melt peaks are shown in Table 4. In both instances, the 30% plasticizer loading run was extended in time, as the extruder barrel was cooled in 5-10 degree °C steps to observe the rise in melt viscosity/drive current. In general, pTSAm allowed processing at ca. 5 degrees lower temperature than the MSM, but the results of the melting peak depression suggest that MSM may have been lost during the extended processing time at elevated temperatures.

Table 4. Thermal analysis of Nylon-11/plasticizer blends at the loading levels indicated (wt/wt). Melting peak of nylon-11 crystallites are reported.

Identity	**Loading**	**pTSAm**	**MSM**
Nylon-11	0	185.9	185.9
Plasticizer	100	136.5	107.6
Nylon-11/plast	30	168.6*	171.9*
Nylon-11/plast	20	172.1	170.7
Nylon-11/plast	~10	180.3*	184.6*
Nylon-11/plast	~7	180.8	180.6

Based on the efficient alloying observed for pTSAm it was selected for processing on the Process 11, an 11mm twin-screw extruder with a higher capacity than the DSM Xplore system. A batch of 350 grams was prepared, comprised of 70% nylon-11 pellets and 30% pTSAm powder. The blend was mixed by hand and then fed into the Process 11 to yield a polymer filament stock, which was subsequently pelletized. The pellets were then combined and fed through the process two additional times to enhance homogenization of the plasticizer in the matrix. Analysis of the resulting masterbatch is pending, and the resulting pellets will be used to conduct formulation and compounding trials with the DSM Xplore system and candidate insect repellents. Yield after three

total passes through the Process 11 was approximately 220 g from the original 350 g, allowing for discarded scrap between material changeover.

6.3. Melt extrusion demonstration

To facilitate development and production of filaments using melt extrusion, DEVCOM-SC successfully produce fibers and filaments on a ca. 100 m scale, which is important to enable demonstrate capability to span the gap from laboratory electrospinning scale (small, nonwoven) to larger, pilot-scale production. In this reporting period, we demonstrate feasibility of the extrusion approach using nylon and LDPE, and also demonstrate successful compounding of permethrin loaded filaments. Specifically, a Xplore Tabletop Extruder equipped with a micro-compounder was used to process polymer filaments ca. 100 m in length and approx. 200 μm in diameter. Polymers were compounded using an Xplore MC40HT micro-compounder which allows for small polymer batch size for processing materials and can process high shear and high viscosity polymers while maintaining good mixing. Furthermore, the micro-compounder affords a consistent dispersion with the incorporation of additives during processing and is capable of processing temperatures up to 425 °C.

As shown in Figure 22, polymer processing was successfully achieved with consistent, uniform filaments produced from nylon and LDPE. For both polymers, the fiber length was approximately 100 m and the fiber diameters ranged from 250-300 μm. Furthermore, nylon-12 with 4 wt% permethrin was also successfully compounded and extruded into 100 m long fibers. This represents feasibility of employing the extruder and compounder to produce fibers of promising fiber designs.

Figure 22. Demonstration of melt extrusion (left), collection onto a spool (center), and spools of composite filaments composed of permethrin-nylon-12, nylon-12, and LDPE (right).

6.4. Conclusions

We evaluated multiple melt depressants and identified pTSAm as a promising additive to effectively reduce the melting point and processing temperature of nylon 12. Concurrently, we demonstrated feasibility to compound and extrude nylon 12, as well as LDPE, at increased scales to produce fibers on the order of 100 m. Together, these findings present significant opportunity to apply findings to progress from electrospinning to incorporate insect repellents into polymer fibers produced using scalable melt extrusion methodology. We intend to incorporate permethrin using the melt depressant to improve processing conditions to evaluate the effect on insect repellent loading and fiber properties.

7. Results and Discussion – FR Nylon Fibers

In this section, we report on the use of electrospinning to fabricate non-woven mats of nylon 66/tannic acid composite nanofibers. Tannic acid was incorporated into nylon nanofibers at concentrations up to 50 wt% while maintaining uniform fiber morphology. Nanofibrous mats were prepared by electrospinning solutions of 12.5 wt% nylon and 0 – 100 wt% tannic acid with respect to nylon. The fibers were characterized using SEM, optical microscopy, ATR-FTIR, DSC, and TGA. The fibers were further characterized using microscale combustion calorimetry (MCC) to determine their heat release properties. Analysis using TGA showed that the tannic acid within the nanofibers begins to degrade at ca. 230 °C and the polymer begins to degrade at ca. 400 °C irrespective of the initial concentration of tannic acid. The char yield increases with respect the concentration of tannic acid, resulting in a maximum of 25% for fibers containing 50 wt% tannic acid. Finally, thermal tests show that tannic acid can still act as an intumescent material when embedded within the nanofibers as the nanofibers are shown to bloom and char under direct heat.

7.1. Concept and Motivation

Nonhazardous flame-retardant materials are of increasing interest as per and polyfluoroalkyl substances (PFAS) and other halogenated flame retardants are being phased out of use due to their associated health and environmental concerns. Tannic acid has emerged as a promising bio-derived, non-toxic, intumescent flame-retardant material. Despite its many advantages, problems with solubility and polymer compatibility have thus far prevented tannic acid from becoming a leading flame-retardant material. Electrospinning provides the opportunity to create flame retardant materials with a unique morphology which can be difficult to achieve using other methods. Finally, electrospun fibers have demonstrated applications in textiles and air

filters, both which would benefit greatly from additional flame-retardant properties.

7.2. Fiber morphology

Table 5. Electrospinning Solution Preparation

Nylon, g	TA, g	[TA] in solution, rel. wt%	[TA] in fibers, theoretical wt %
1.25	0	0	0
1.25	0.125	10.0	9.0
1.25	0.375	30.0	23.1
1.25	0.625	50.0	33.3
1.25	0.937	75.0	42.8
1.25	1.25	100	50.0

Nanofibers were prepared by electrospinning solutions of nylon in formic acid with 0-100 wt% TA with respect to nylon (rel. wt%). Samples were prepared by dissolving 1.25 grams of nylon into 10 g solution to achieve a nylon concentration of 12.5 wt%. Then 0-1.25 g of TA was added to achieve final concentrations of 0, 10, 30, 50, 75 and 100 rel. wt% TA (Table 5). The solutions were sealed and heated at 60 °C overnight to dissolve the contents. After overnight heating, nylon and TA completely dissolved at all concentrations prepared. Solutions were thoroughly mixed by vortexing before electrospinning and stored for up to one week at 2-4 °C. Fibrous mats were prepared from solutions containing ≤ 50 rel. wt% TA at 15 cm and 15 kV, but at ≥75 rel. wt%, a higher voltage was necessary, and the polymer would solidify on the needle tip requiring routine cleaning during the electrospinning process. Non-woven mats were collected for 2-6 hours resulting in solid nanofibrous mats at all concentrations of TA tested. An example of a fibrous mat made from a solution containing 100 rel. wt% TA is given in Figure 23.

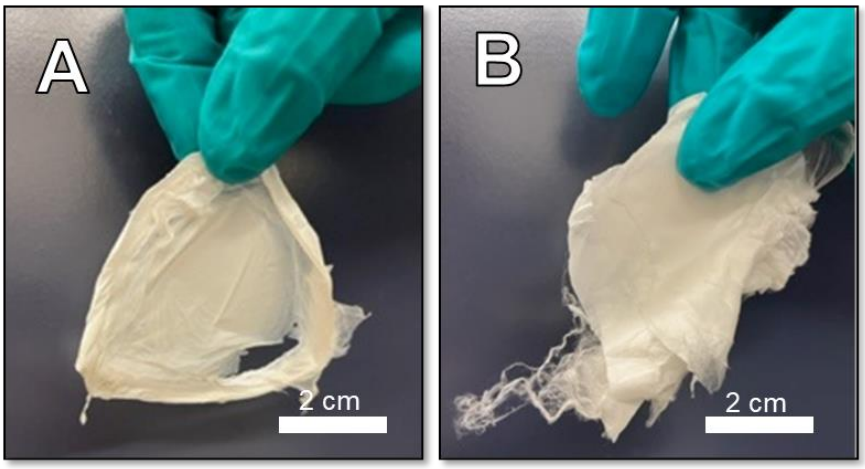

Figure 23. Images of nanofibrous mats containing 10 (A) and 100 (B) rel. wt% TA.

Fibrous mats were analyzed using SEM and optical microscopy (Figure 24) and compared to neat nylon nanofibers. Uniform, defect-free fibers were obtained regardless of TA loading. In the absence of TA, electrospinning resulted in a non-woven mat of ca. 100 nm fibers and the only noticeable effect of increasing TA concentration is a gradual increase in fiber diameter. With up to 30 rel. wt% TA, there is little effect on fiber diameter as all fibers measure ca. 120 nm. At > 50 rel. wt% TA there is a modest increase in fiber diameter to 258 ± 93 nm at 50 rel. wt% and 439 ± 86 nm at 75 rel. wt% and a diameter of 656 ± 113 nm at 1:1 nylon/TA. Despite the increase in fiber diameter caused by increasing amounts of TA, all fibers remain cylindrical with few defects. Previous studies have shown that nylon fibers can collapse into ribbons at high (ca. >500 nm) fiber diameters due to the rapid solvent loss during electrospinning and subsequent collapse of thin fiber walls, however we do not observe significant ribbons in our study suggesting that TA provides some structure to the polymer network during the electrospinning process[60].

Optical microscopy images of nylon fibers containing 100 rel. wt% TA are given in Figure 24 at three different scales. The uniformity of the non-woven mat can be seen in the microscopy images. The edge of the mat illustrating the non-woven and highly porous nature of the materials is given in Figure 24D. The mat is comprised of a uniform distribution of nanofibers,

even at high (1:1) TA loadings. As shown in images at higher magnification (Figure 24E, F), there are no visible defects in the fiber morphology. Neat nylon is an optically clear material and, surprisingly, the fibers are still relatively clear at 100 rel. wt% TA loadings. The uniformity of the fibers suggest that the TA is evenly distributed within the polymer matrix. If the components were incompatible with one another, one would expect some phase separation during electrospun leading to beaded or otherwise non-uniform fibers. However, the high solubility of both TA and nylon in the electrospinning solution suggests that the two materials are highly compatible with one another resulting in remarkably uniform cylindrical fiber morphologies, even at extremely high TA loadings.

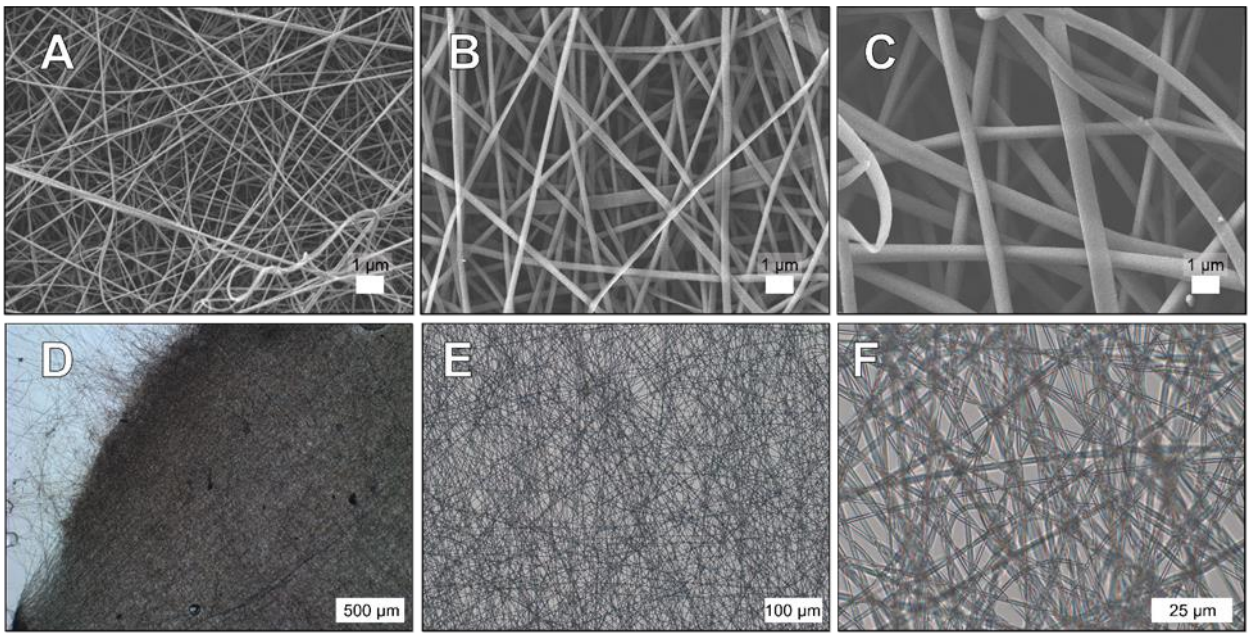

Figure 24. There is a general increase in fiber morphology with the addition of tannic acid as shown by SEM images of fibers made with 0 (A), 50 (B) and 100 (C) rel. wt% TA (Scale bar = 1 µm). Fiber morphology and uniform incorporation of TA can be further verified by optical microscopy of a fibrous mat made with 100 rel. wt% TA as shown at three different magnifications (D-F).

Table 6. Electrospun Fiber Diameters

[TA], rel. wt%	**Diameter, nm[a]**
Neat	119 ± 34
10	115.0 ± 15
30	130 ± 15
50	258 ± 93
75	439 ± 86
100	656 ± 113

[a] *Determined using Image J based on SEM images with n ≥ 100*

The structural composition of Nylon/TA fibers was investigated using ATR-FTIR. Neat TA (Figure 25, Red) has characteristic absorbance peaks at 1004 cm^{-1}, 1161 cm^{-1}, a CH_2 aromatic stretch at 1598 cm^{-1}, a carbonyl stretch at 1694 cm^{-1} (ν_s (C=O)) and a broad OH stretch at ca. 3300 cm^{-1} corresponding to the phenols. Neat nylon (Figure 25, Black) exhibits a characteristic sharp N-H stretch centered at 3300 cm^{-1}, peak corresponding to CH_2 stretches at 2933 ($\nu_s(CH_2)$ asymmetric) and 2860 cm^{-1} ($\nu_s(CH_2)$ symmetric) and amide stretches at 1636 cm^{-1} (amide I, ν_s(CO), 1536 cm^{-1} (amide II, ν_s(NH), and 1275 cm^{-1} (amide III). Spectra of Nylon/TA composite fibers indicate even distribution of TA within the polymer matrix. Spectra of nanofibers containing 10 and 100 rel. wt% TA are given in Figure 25. With increasing concentration of TA, there is a corresponding increase in the characteristic TA peaks discussed above. At 100 rel. wt%, peaks corresponding to TA and nylon are visible in relatively equal intensity. The CH_2 stretches for nylon at ca. 2900 cm^{-1} and the OH stretch for TA at ca. 3300 cm^{-1} are unshifted in the composite relative to neat starting materials, however, the nylon amide stretches are compressed, and the TA carbonyl stretch shifts to 1708 cm^{-1} in the composite fibers. Shifts in the amide and carbonyl regions indicate interactions between the polar amide regions of nylon and the aromatic esters on TA further suggesting that TA is interspersed within the nylon matrix and does not exist in phase-separated regions.

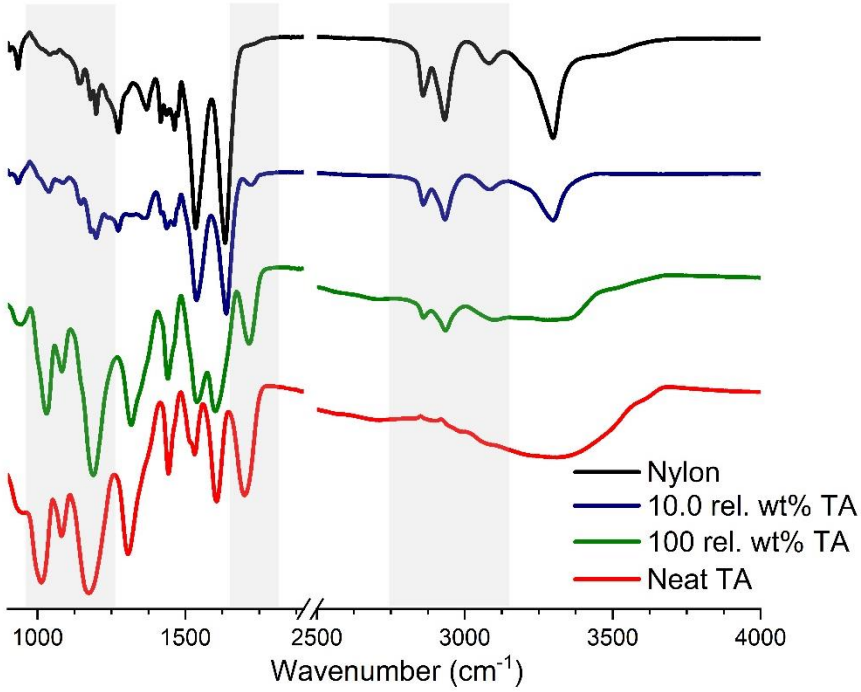

Figure 25. ATR-FTIR of Electrospun nanofibers. The characteristic regions are highlighted in grey. Nylon/TA composites are shown at 10 rel. wt% (Blue) and 100 rel. wt% (green).

7.3. Thermal Analysis

Thermal analysis of nanofibrous mats was performed in N_2 and air using TGA from ambient to 600 °C (Figure 26). A summary of the thermal properties is provided in Table 7. Under nitrogen, there is a single weight loss for neat nylon at 422 °C corresponding to its thermal decomposition and composite fibers show an additional weight loss peak at ca. 250 °C corresponding to the decomposition of TA. When compared with neat nylon, incorporation of TA does not negatively affect its peak thermal decomposition temperature. Indeed, at 100 rel. wt% TA, nylon decomposes at 421 °C indicating that the incorporation of high concentrations of TA have little effect on the stability of the polymer matrix. The residual mass at 375 °C gives an indication of the TA loading in the electrospun fibers as the nylon has not yet degraded and indicated that much of the TA loaded into the electrospinning solution is incorporated into the

polymer fibers. Finally, the residual mass at 600 °C gives an estimation of the char-forming ability of the material. With increasing TA loadings, there is an increase in the residual mass. There is no residual mass for neat nylon, but at only 10 rel. wt% there is an increase to 7.8% mass remaining. The residual mass continues to increase with TA loadings resulting in a maximum of 20.2% remaining for 100 rel. wt% TA. The residual mass is an indication that the TA is still able to char and act as an intumescent material when dispersed within the polymer network. Additionally, a char yield of ≥20% indicates good fire resistance.

Thermal analysis was also performed in air for 10 and 100 rel. wt% TA fibers. In air, there is little effect on the thermal decomposition of nylon, or TA, but there was no residual mass at 600 °C. The lack of residual mass under air is expected due to thermal oxidation reactions. Importantly, however, the TGA curves in air and nitrogen are otherwise near superimposable indicating that the presence of oxygen does not affect the properties of nylon/TA composite fibers.

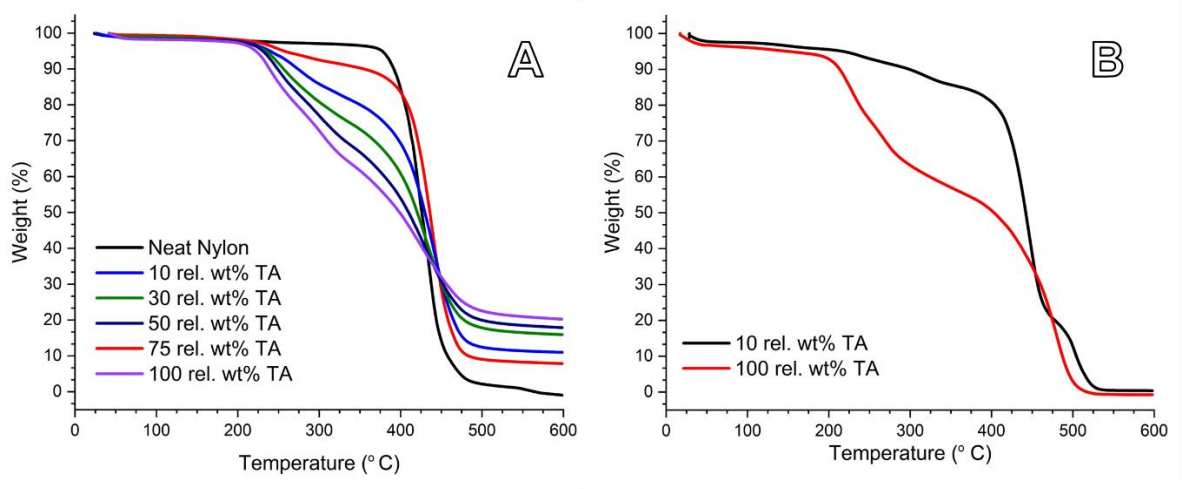

Figure 26. *Left*: TGA ramps of nylon nanofibers with 0 – 100 rel. wt% TA under N_2. *Right*: TGA ramps of nylon nanofibers with 10 and 100 rel. wt% TA heated from ambient to 50 °C under N_2 before switching the atmosphere to air.

Table 7. Thermal Properties of Electrospun Fibers

[TA], rel. wt%	**$T_{onset\ 10\%}$ (°C)[a]**	**T_{max1} (°C)[b]**	**T_{max2} (°C)[c]**	**Residual Mass at 375 °C (%)[d]**	**Residual Mass at 600 °C (%)[e]**
Neat	390	422	-	95.3	0.0
10	354	247	438	88.4	7.84
30	273	272	439	76.0	11.0
50	252	255	432	68.2	15.9
75	248	247	430	61.2	17.9
100	238	238	421	56.3	20.2

[a] Recorded as the residual mass after heating to 600 °C under N_2 as measured by TGA. [b] Temperature at first maximum weight loss rate. [c] Temperature at second maximum weight loss rate. [a-e] Under N_2.

The heat release properties of nylon/TA composite fibers were further analyzed by MCC. The heat release capacity decreased significantly with the addition of TA. At 10 rel. wt.%, the heat release capacity decreased by 32% from 626 to 424 $J \bullet g^{-1} \bullet K^{-1}$, respectively, when compared with neat nylon. The heat release capacity continues to decrease with increasing TA until at ≥75 rel. wt% TA, it drops below the minimum value of 200 $J \bullet g^{-1} \bullet K^{-1}$ to be considered flame resistant with an ultimate reduction in heat capacity of 74% for 100 rel. wt% TA. Likewise, the THR decreases significantly with increasing TA. The decrease starts to become significant at 30 rel. wt% TA loading with a decrease of 22% in THR and becomes more prominent for 75 and 100 rel. wt% TA with a decrease of 42 and 46%, respectively. These results further demonstrate the impact on the flame resistance of nylon, turning what started as a flammable polymer into a flame-retardant composite. These data are comparable to some of the most recent TA-based flame-retardant materials and coatings and demonstrate the feasibility of this technique for preparing flame retardant nylon composites[43].

7.4. Flame tests

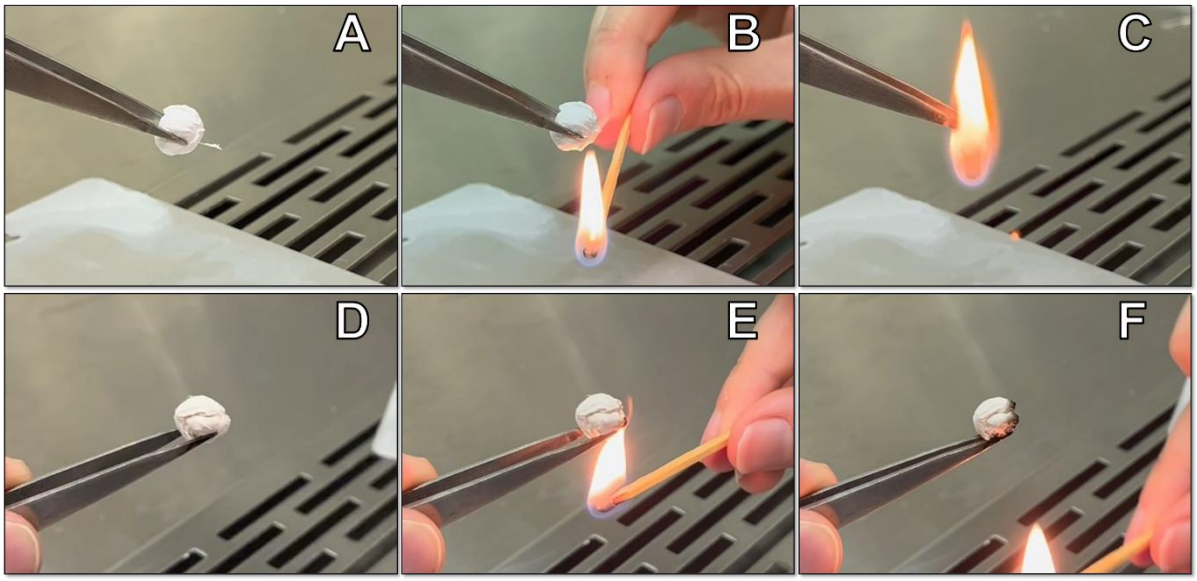

Figure 27. Exposure of nanofibrous mats to an open flame. The mats were directly exposed for ca. 2 seconds before the ignition source was removed. Results are shown for mats without TA (A-C) and with 100 rel. wt% TA (D-F). (A, D) Before ignition. (B,E) During flame exposure. (C-F) Images taken 10 seconds after exposure.

Compressed fibrous mats weighing 100-200 mg and measuring ca. 1 x 1 cm were exposed to an open flame to investigate their performance. As previously mentioned, nylon will melt, drip, and generally shrink away from the ignition source without charring. This can be seen in Figure 27A-C which shows the exposure of a nanofibrous nylon mat to an open flame source. Seconds after exposure, the mat ignites and burns rapidly. During combustion, there are flaming drops of melted polymer that fall from the burning sample until there is no remaining residue (Figure 27C). Exposure of a fibrous mat with 75 rel. wt% TA to an open flame results in combustion, but without afterglow, dripping, and is almost immediately extinguished. The exposed area significantly chars, leaving the unexposed area essentially unaffected. At 100 rel. wt%, the polymer does not combust and is only minimally affected by open flame exposure (Figure 27D-F). The charred area remains small and completely insulates the unexposed areas of the fibrous mat. Any ignition is immediately extinguished without afterglow and no melt-dripping. A summary of open flame tests for fibrous

mats is given in Table 8.

Table 8. Flame Resistance of Nanofibrous Mats

[TA], rel. wt%	**Heat Release Capacity [a], $J \cdot g^{-1} \cdot K^{-1}$**	**THR [a], $kJ \cdot g^{-1}$**	**Combustion**	**Afterglow**	**Drip**	**Extinguishment**
0	626	27.6	YES	YES	YES	NO
10	424	26.0	-	-	-	-
30	317	21.5	-	-	-	-
50	248	18.2	-	-	-	-
75	197	16.0	YES	NO	NO	YES
100	165	12.7	NO	NO	NO	YES

[a] *Average of three measurements.*

7.5. FR Nylon Conclusions

Electrospinning was used to formulate and evaluate the efficacy of tannic acid as a fire-retardant additive in nylon fiber compositions. Importantly, electrospinning enabled the very high loading (up to 1:1 ratio) of tannic acid in nylon and maintain fiber morphology. Tannic acid was shown to be an effective fire-retardant additive for nylon fibers. At tannic acid loading levels greater than 75 rel. wt%, heat release values exceeding the required minima for acceptable FR levels were attained. The FR behavior as indicated by thermal analysis was confirmed using open flame tests, where the TA-nylon fibers resisted burning with exposure to open flame. The mechanism of FR imparted by TA into nylon appeared to be intumescent char formation from the TA components. The FR nonwoven TA-nylon mats have potential to serve as standalone FR materials in various applications, and also importantly serves as a prototype to show feasibility for using TA in nylon fibers produced through more scalable approaches, such as melt extrusion.

8. Summary and Conclusions

8.1. Summary

In year 2, we have made substantial progress in Tasks 1, 3, and 4, which correspond to electrospun prototyping, scalable extrusion, and multifunctional fibers, respectively. In Task 1, we developed mixed insect repellent-doped recycled polyethylene terephthalate (PET) electrospun microfibers and demonstrated their efficacy using a novel live insect bioassay specifically designed for insect repellent loaded textiles. In task 3, we made progress in two parallel scalable fiber fabrication pathways, dry jet wet spinning and melt extrusion. We identified and employed the benefits of dry jet wet spinning, which extrudes polymer gels at relatively low temperatures that enables the incorporation of volatile repellents, to a novel polymer-DEET gel formulation that has significant promise to serve as a fiber core, as well as standalone repellent material. For melt extrusion, we identified a promising melt depressant that effectively lowers the processing temperature of nylon to enable compatibility with insect repellents. Towards Task 4, we designed, formulated, and tested flame retardant tannic acid-nylon fibers that demonstrated the natural product tannic acid as an effective fire-retardant additive for nylon. We will build upon these findings in year 3 to incorporate insect repellency for a multifunctional fiber proof of concept.

8.2. Significance

In this reporting period, we presented several advancements in the program that have potential to serve as standalone insect repellent materials, will enable future development insect repellent loaded fibers and textiles, and provide significant contribution to the field. The nonwoven fibrous mats sourced from recycled PET consumer goods have the capability to function as patches for long-term repellent release to repel biting arthropods from exposed skin.

Furthermore, the high affinity between DEET and PET we identified will be leveraged in the design of future filaments. Our development and demonstration of a novel bioassay specifically designed to evaluate the repellency of insect repellent loaded fibers and textiles will have significant implications for providing live insect performance on materials developed in Y3 of this program, as well as provide new and useful methods to others in the field. Our design and formulation of insect repellent loaded-polymer gels has potential for significant impact as standalone insect repellent materials (passive-release or thermally induced repellent beads, strings, gels), as well as to serve as a highly loaded core in bicomponent fiber designs. Importantly, the gel designs are compatible with dry jet wet spinning, which is a scalable, manufacturing compatible extrusion method. We also identified a promising melt depressant to lower the processing temperatures of nylon to enable volatile repellent incorporation to improve the compatibility of insect repellents with conventional melt extrusion manufacturing, which represents a promising transition pathway for textile applications.

8.3. Next steps

Moving forward to year 3, we will continue to build upon the findings of years 1 and 2 to deliver new insect repellent and multifunctional fiber technologies. Our goals are to continue to deliver advanced technology readiness (TRL) prototypes by application of the novel bioassay, down select and focus on designs compatible with scalable fiber production methods, deliver a swatch prototype, and engage with commercial transition partners to pursue a EPA registration pathway. For the P(AN-VC)/DEET gels, we will evaluate and demonstrate the standalone release kinetics and live-insect repellency to demonstrate potential use as standalone gel-based materials. Furthermore, the P(AN-VC)/DEET gels will be incorporated into bicomponent fibers through dry

jet wet spinning to serve as the core of a core-sheath design with potential for long-lasting insect repellency from EPA-registered DEET. We will focus heavily on melt extruded fiber production, as melt extrusion is the most scalable, cost-effective fiber production method which facilitates transition to commercial production. We will leverage our findings in melt depressants to incorporate insect repellents, such as permethrin, into nylon-12 fibers. We aim to down select a best performing formulation to extrude, produce yarns, and ultimately deliver a knit swatch prototype to represent advanced TRL. Finally, we will use leverage our findings from Y2 tannic acid-nylon fibers to design and evaluate multifunctional fibers that exhibit long-term insect repellency and fire-retardant behavior that will represent a new class of environmentally friendly high-performance fibers for textile applications.

References

1. Fighting the World's Deadliest Animal. **2019**.

2. Breedlove, B. Deadly, Dangerous, and Decorative Creatures. *Emerging Infectious Diseases* **2022,** *28*, 495-495.

3. *Global vector control response 2017–2030*. World Health Organization.

4. Organization, W. H. *World malaria report 2022*; World Health Organization: **2022**.

5. Bhatt, S.; Weiss, D. J.; Cameron, E.; Bisanzio, D.; Mappin, B.; Dalrymple, U.; Battle, K.; Moyes, C. L.; Henry, A.; Eckhoff, P. A.; Wenger, E. A.; Briet, O.; Penny, M. A.; Smith, T. A.; Bennett, A.; Yukich, J.; Eisele, T. P.; Griffin, J. T.; Fergus, C. A.; Lynch, M.; Lindgren, F.; Cohen, J. M.; Murray, C. L. J.; Smith, D. L.; Hay, S. I.; Cibulskis, R. E.; Gething, P. W. The effect of malaria control on Plasmodium falciparum in Africa between 2000 and 2015. *Nature* **2015,** *526*, 207-211.

6. Jadhav, S.; Sirdesai, A.; Bandyopadhyay, a. P. Assessment of comparative bio-efficacy of mosquito repellent cream and liquid mosquito repellent vaporizers. *International Journal of Mosquito Research* **2022,** *9*, 44-46.

7. Santos, J. d.; Lourenco, R. L.; Rosa, P.; Adams, A. I. H. Evaluation of quality and safety parameters of DEET commercial repellents photostability , penetration/permeation and eye irritation studies. *Drug Analytical Research* **2022,** *6*, 21-26.

8. Jinchan, J.; Gong, Y.; An, Z.; Li, M.; Huo, Y.; Zhou, Y.; Jin, Z.; Xie, J.; He, M. Theoretical investigation on degradation of DEET by• OH in aqueous solution: Mechanism, kinetics, process optimization and toxicity evaluation. *Journal of Cleaner Production* **2022,** *362*, 132260.

9. Katz, T. M.; Miller, J. H.; Hebert, A. A. Insect repellents: historical perspectives and new developments. *J Am Acad Dermatol* **2008,** *58*, 865-71.

10. Ryan, J. J.; Casalini, R.; Orlicki, J. A.; Lundin, J. G. Controlled release of the insect repellent picaridin from electrospun nylon-6,6 nanofibers. *Polym Advan Technol* **2020,** *31*, 3039-3047.

11. Strid, A.; Hanson, W.; Cross, S.; Bond, C.; Jenkins, J., Insect Repellents Fact Sheet. National Pesticide Information Center, Oregon State University Extension Services: **2018**.

12. Prevent Mosquito Bites. **2022**.

13. Goodyer, L.; Schofield, S. Mosquito repellents for the traveller: does picaridin provide longer protection than DEET. *Journal of Travel Medicine* **2018,** *25*, S10-S15.

14. Dennis, E. J.; Goldman, O. V.; Vosshall, L. B. Aedes aegyti Mosquitoes use their legs to sense DEET on contact. *Current Biology* **2019,** *29*, 1551-1556.

15. Elsayed, G. A.; Hassabo, A. G. Insect repellent of cellulosic fabrics (A Review). *Letters in Applied NanoBioScience* **2022,** *11*, 3181-3190.

16. Mapossa, A. B.; Focke, W. W.; Tewo, R. K.; Androsch, R.; Kruger, T. Mosquito-repellent controlled-release formulations for fighting infectious diseases. *Malaria Journal* **2021,** *20*, 1-33.

17. Shah, S. I.; Khutoryanskiy, V. V.; Williams, A. C. A Novel Polymer Insect Repellent Conjugate for Extended Release and Decreased Skin Permeation of Para-Menthane-3,8-Diol. *Pharmaceutics* **2021,** *13*, 403.

18. Iscan, Y.; Hekimoglu, S.; Sargon, M. F.; Hincal, A. A. DEET-loaded solid lipid particles for skin delivery: In vitro release and skin permeation characteristics in different vehicles. *Journal of Microencapsulation* **2005,** *23*, 315-327.

19. Kadam, S. L.; yadav, P.; Bhutkar, S.; Patil, V. D.; Shukla, P. G.; Shammuganathan, K. Sustained release insect repellent microcapsules using modified cellulose nanofibers (mCNF) as pickering emulsifier. *Colloids and Surfaces A: Physicochemical and Engineering Aspects* **2019,** *582*, 123883.

20. Maia, J. D.; Corte, R. L.; Martinez, J.; Ubbink, J.; Prata, A. S. Improved activity of thyme essential oil (Thymus vulgaris) against Aedes aegypti larvae using a biodegradable controlled release system. *Industrial Crops and Products* **2019,** *136*, 110-120.

21. Sibanda, M.; Focke, W.; Braack, L.; Leuteritz, A.; Brünig, H.; Tran, N. H. A.; Wieczorek, F.; Trümper, W. Biocomponent fibres for controlled release of volatille mosquito repellents. *Materials Science and Engineering: C* **2018,** *91*, 754-761.

22. Ahang, J.; Xiao, C.; Lin, Y.; Yang, H.; Zhang, Y. S.; Ding, J. An oxidative stress-responsive electrospun polyester membrane capable of releasing anti-bacterial and anti-inflaammatroy agents for postoperative anti-adhesion. *Journal of Controlled Release* **2021,** *335*, 359-368.

23. Thum, M. D.; Weise, N. K.; Casalini, R.; Fulton, A. C.; Purdy, A. P.; Lundin, J. G. Incorporation of N,N,-diethyl-meta-toluamide within electrospun nylon-6/6 nanofibers. *Journal of Applied Polymer Science* **2022,** *139*, e53237.

24. Ryan, J. J.; Casalini, R.; Orlicki, J. A.; Lundin, J. G. Controlled release of the insect repellent picaridin from electrospun nylon-6,6 nanofibers. *Polymer Advanced Technologies* **2020,** *31*, 3039-3047.

25. Muñoz, V.; Buffa, F.; Molinari, F.; Hermida, L. G.; García, J. J.; Abraham, G. A. Electrospun ethylcellulose-based nanofibrous mats with insect-repellent activity. *Materials Letters* **2019,** *253*, 289-292.

26. Bonadies, I.; Longo, A.; Androch, R.; Jehnichen, D.; Gobel, M.; Lorenzo, M. L. D. Biodegradable electrospun PLLA fibers containing the mosquito-rperllent DEET. *European Polymer Journal* **2019,** *113*, 377-384.

27. Bumbudsanpharoke, N.; Ko, S. Nanoclays in Food and Beverage Packaging. *Journal of Nanomaterials* **2019**.

28. Phaln, A.; Meissner, K.; Humphrey, J.; Ross, H. Plastic Pollution and packaging: Corporate commitments and actions drom the food and beverage sector. *Journal of Cleaner Production* **2022,** *331*, 129827.

29. Milbrandt, A.; Coney, K.; Badgett, A.; Beckman, G. T. Quantification and evaluation of plastic waste in the United States. *Resourrces, Conservation and Recycling* **2022,** *183*, 106363.

30. Strain, I. N.; Wu, Q.; Pourrahimi, A. M.; Hedenqvist, M. S.; Olsson, R. T. Electrospinning recycled PET to generate tough mesomorphic fibre membranes for smoke filtration. *Journal of Materials Chemistry A* **2015,** *3*, 1632.

31. Jin, X.; Wei, C. X.; Wu, C. W.; Zhang, W. Customized Hydrogel for Sustained Release of Highly Water-Soluble Drugs. *Acs Omega* **2022,** *7*, 8493-8497.

32. Mullarney, M. P.; Seery, T. A. P.; Weiss, R. A. Drug diffusion in hydrophobically modified N,N-dimethylacrylamide hydrogels. *Polymer* **2006,** *47*, 3845-3855.

33. Tong, X. M.; Lee, S.; Bararpour, L.; Yang, F. Long-Term Controlled Protein Release from Poly(Ethylene Glycol) Hydrogels by Modulating Mesh Size and Degradation. *Macromol Biosci* **2015,** *15*, 1679-1686.

34. Lin, K. Y.; Wang, D. M.; Lai, J. Y. Nonsolvent-induced gelation and its effect on membrane morphology. *Macromolecules* **2002,** *35*, 6697-6706.

35. Jimenez, J.; Ford, E. Mapping wet vs gel spinning in Hansen space. *Polymer* **2021**, 124079.

36. Xue, J. J.; Wu, T.; Dai, Y. Q.; Xia, Y. N. Electrospinning and Electrospun Nanofibers: Methods, Materials, and Applications. *Chem Rev* **2019,** *119*, 5298-5415.

37. Kim, C.; Jeong, Y. I.; Ngoc, B. T. N.; Yang, K. S.; Kojima, M.; Kim, Y. A.; Endo, M.; Lee, J. W. Synthesis and characterization of porous carbon nanofibers with hollow cores through the thermal treatment of electrospun copolymeric nanofiber webs. *Small* **2007,** *3*, 91-95.

38. Li, D.; Xia, Y. N. Direct fabrication of composite and ceramic hollow nanofibers by electrospinning. *Nano Lett* **2004,** *4*, 933-938.

39. McCann, J. T.; Marquez, M.; Xia, Y. N. Highly porous fibers by electrospinning into a cryogenic liquid. *J Am Chem Soc* **2006,** *128*, 1436-1437.

40. Rezabeigi, E.; Wood-Adams, P. M.; Demarquette, N. R. Complex Morphology Formation in Electrospinning of Binary and Ternary Poly(lactic acid) Solutions. *Macromolecules* **2018,** *51*, 4094-4107.

41. Tian, X. L.; Bai, H.; Zheng, Y. M.; Jiang, L. Bio-inspired Heterostructured Bead-on-String Fibers That Respond to Environmental Wetting. *Adv Funct Mater* **2011,** *21*, 1398-1402.

42. Zhao, Y.; Cao, X. Y.; Jiang, L. Bio-mimic multichannel microtubes by a facile method. *J Am Chem Soc* **2007,** *129*, 764-765.

43. Kulkarni, S.; Xia, Z. Y.; Yu, S. R.; Kiratitanavit, W.; Morgan, A. B.; Kumar, J.; Mosurkal, R.; Nagarajan, R. Bio-Based Flame-Retardant Coatings Based on the Synergistic Combination of Tannic Acid and Phytic Acid for Nylon-Cotton Blends. *Acs Appl Mater Inter* **2021,** *13*, 61620-61628.

44. Lei, T. Y.; Chen, W.; Hu, Y.; Lv, W. Q.; Lv, X. X.; Yan, Y. C.; Huang, J. W.; Jiao, Y.; Chu, J. W.; Yan, C. Y.; Wu, C. Y.; Li, Q.; He, W. D.; Xiong, J. A Nonflammable and Thermotolerant Separator Suppresses Polysulfide Dissolution for Safe and Long-Cycle Lithium-Sulfur Batteries. *Adv Energy Mater* **2018,** *8*.

45. Selvakumar, N.; Azhagurajan, A.; Natarajan, T. S.; Khadir, M. M. A. Flame-retardant fabric systems based on electrospun polyamide/boric acid nanocomposite fibers. *J Appl Polym Sci* **2012,** *126*, 614-619.

46. Vahabi, H.; Wu, H.; Saeb, M. R.; Koo, J. H.; Ramakrishna, S. Electrospinning for developing flame retardant polymer materials: Current status and future perspectives. *Polymer* **2021,** *217*.

47. Zhou, Z. F.; Chen, B. B.; Fang, T. T.; Li, Y.; Zhou, Z. F.; Wang, Q. J.; Zhang, J. J.; Zhao, Y. F. A Multifunctional Separator Enables Safe and Durable Lithium/Magnesium-Sulfur Batteries under Elevated Temperature. *Adv Energy Mater* **2020,** *10*.

48. Xia, Z. Y.; Kiratitanavit, W.; Facendola, P.; Yu, S. R.; Kumar, J.; Mosurkal, R.; Nagarajan, R. A Bio-derived Char Forming Flame Retardant Additive for Nylon 6 Based on Crosslinked Tannic Acid. *Thermochim Acta* **2020,** *693*.

49. Xia, Z. Y.; Singh, A.; Kiratitanavit, W.; Mosurkal, R.; Kumar, J.; Nagarajan, R. Unraveling the mechanism of thermal and thermo-oxidative degradation of tannic acid. *Thermochim Acta* **2015,** *605*, 77-85.

50. Hagerman, A. E.; Riedl, K. M.; Jones, G. A.; Sovik, K. N.; Ritchard, N. T.; Hartzfeld, P. W.; Riechel, T. L. High molecular weight plant polyphenolics (tannins) as biological antioxidants. *J Agr Food Chem* **1998,** *46*, 1887-1892.

51. Jiang, S.; Yang, L.; Bloomquist, J. R. High-throughput screening method for evaluating spatial repellency and vapour toxicity to mosquitoes. *Medical and Veterinary Entomology* **2019,** *33*, 388-396.

52. Owusu, H. F.; Müller, P. How important is the angle of tilt in the WHO cone bioassay? *Malaria Journal* **2016,** *15*, 243.

53. Koombhongse, S.; Liu, W.; Reneker, D. H. Flat polymer ribbons and other shapes by electrospinning. *J. Polym. Sci., Part B: Polym. Phys.* **2001,** *39*, 2598-2606.

54. Fond, H.; Reneker, D. H. Elastomeric nanofibers of styrene-butadiene-styrene triblock

copolymer. *Polymer Science Part B: Polymer Physics* **1999,** *37*, 3488-3493.

55. Knepper, T. P. Analysis and mass sppectrometric characterization f the insect repellent Bayrepel and its main metabolite Bayrepel-acid. *Journal of Chromatography A* **2004,** *1046*, 159-166.

56. Park, S.; Thanokkasaranee, S.; Shin, H.; Lee, Y.; Tak, G.; Seo, J. PET/Bio-Based Terpolyester Blends with High Dimensional Thermal Stability. *Polymers* **2021,** *13*, 728.

57. Rowley, W. A.; Graham, C. The effect of temperature and relative humidity on the flight performance of female Aedes aegypti. *Journal of Insect Physiology* **1968,** *14*, 1251-1257.

58. Tavares, M.; Silva, M. R. M. d.; Siqueira, L. B. d. O. d.; Rodrigues, R. A. S.; Bodjolle-d'Almeida, L.; Santos, E. P. d.; Ricci-Júnior, E. Trends in insect repellent formulations: A review. *International Journal of Pharmaceutics* **2018,** *539*, 190-209.

59. Sixta, H.; Michud, A.; Hauru, L.; Asaadi, S.; Ma, Y.; King, A. W. T.; Kilpeläinen, I.; Hummel, M. Ioncell-F: A High-strength regenerated cellulose fibre. *Nord. Pulp Pap. Res. J.* **2015,** *30*, 43-57.

60. Koombhongse, S.; Liu, W. X.; Reneker, D. H. Flat polymer ribbons and other shapes by electrospinning. *Journal of Polymer Science Part B-Polymer Physics* **2001,** *39*, 2598-2606.